Study on the Effect of Pre-corrosion on Crack Initiation and Fatigue Life of an Aluminum Alloy

Thesis Submitted in Partial Fulfillment
of the Requirements for the Award of

Master of Technology
in
Machine Design and Analysis
by

Vaneshwar kumar Sahu
Roll No: 207ME105

Department of Mechanical Engineering
National Institute of Technology
Rourkela
2009

Study on the Effect of Pre-corrosion on Crack Initiation and Fatigue Life of an Aluminum Alloy

Thesis Submitted in Partial Fulfillment
of the Requirements for the Award of

Master of Technology
In
Machine Design and Analysis
By

Vaneshwar kumar Sahu
Roll No: 207ME105

Under the Guidance of

Prof. P.K. RAY
Prof. B.B. VERMA

Department of Mechanical Engineering
National Institute of Technology
Rourkela
2009

National Institute of Technology
Rourkela

CERTIFICATE

This is to certify that the thesis entitled, **"Study on the Effect of Pre-corrosion on Crack Initiation and Fatigue Life in an Aluminum Alloy"** submitted by **Mr. Vaneshwar kumar Sahu** in partial fulfillment of the requirements for the award of **Master of Technology** Degree in **Mechanical Engineering** with specialization in **Machine Design and Analysis** at the National Institute of Technology, Rourkela (Deemed University) is an authentic work carried out by him under our supervision and guidance.

To the best of our knowledge, the matter embodied in the thesis has not been submitted to any other University/ Institute for the award of any degree or diploma.

Prof. P.K. Ray
Dept. of Mechanical Engg.
National Institute of Technology
Rourkela - 769008

Prof. B.B. Verma
Dept. of Metallurgical and Materials Engg.
National Institute of Technology
Rourkela - 769008

Date:

Contents

ACKNOWLEDGEMENT

This course of time made me to improve my personal knowledge and skill. I feel the need to thank people who let this journey pleasant and a fruitful.

First of all I am thankful to Dr .P.K. Ray and Dr. B.B. Verma for their inspiration for taking up this project and guidance throughout my project work. The way they taught me can never be forgettable and their timely suggestions are precious. I also express my sincere gratitude to Prof. R. K. Sahoo, Head of the Department, Mechanical Engineering, for providing valuable departmental facilities. I would like to acknowledge Mr. Jyothi Ranjan Mohanthy and Ms. Archana Mallik for their continuous support during this course of time.

And I also want to say thanks to Mr. S. Hembram, Mr. Rajesh Patnaik, Mr. Sameer Pradhan and Mr. K.C. Das for their cooperation in their respective labs.

I am thankful to my parents for their love and pushup in this course of time and I am thankful to almighty for giving me an opportunity to join in this institute.

Finally I would like to show my sincere gratitude to one and all the people who helped me throughout this project without whom this work can't be materialized.

Vaneshwar kumar Sahu

Roll no 207ME105

Dept. of Mechanical Engineering

National Institute of Technology, Rourkela

Abstract

Corrosion leading to fatigue crack nucleation and crack growth is considered to be among the most significant degradation mechanisms in aging structures. Especially in aircrafts, widespread corrosion pits on the surface and hidden within the joints are an important cause for damage since fatigue cracks are observed to nucleate and propagate from these corrosion pits.

It is known that fatigue properties of any material depend on the homogeneity of the material mostly the surface uniformity. Any irregularity present may cause fatigue crack initiation at a stress comparably lower than that shown in a homogeneous material. Fatigue life estimation in stress controlled condition is done by conducting Moore test. The environmental exposure of aluminum alloys generally shifts the curve to a lower stress region and reduction in life. In several cases *S-N* curve of pre-corroded condition shows some lowering of the curve from the original one due to the presence of corrosion pits [15]. The effect of corrosion in fatigue life of pre-corroded 7020-T7 aluminum alloy has been studied and presented in this investigation.

As the fatigue failure process exploits the weakest links (discontinuities) within the test material, which act as nucleation sites for crack origins, the fatigue properties of un-corroded and pre-corroded 7020-aluminum alloy in 3.5% NaCl have been studied and compared in this project. The criteria being the *S-N* curve, fatigue life, endurance limit, corrosion mechanism, stress concentration factor, SEM fractograph and probable crack initiation cause and spot.

Round specimen generally used in classical fatigue tests for endurance limit estimation have been used in this experiment. S-N curve is plotted by using Moore's rotating cantilever beam type fatigue testing machine. The tests are conducted in un-corroded specimen and in pre-corroded specimen and then results are compared. Also the spot of crack initiation is predicted by using fractographs under SEM. The pit dimensions are measured using an elliptical model and a relation between stress intensity factor and life is plotted.

The results of the experiment confirm the findings of literatures referred, along with that, the fatigue and crack initiation behavior of pre-corroded 7020-Al alloy has been found experimentally.

List of figures: Page No.

List of tables: Page No.

Nomenclature

σ	Applied stress
x,y	Coordinate axes
ρ	Radius of curvature at notch
c	Semi-major axis of ellipse
b	Semi-minor axis of ellipse
K_t	Theoretical stress concentration factor
Ψ	Elliptical integral
ϕ	Angle between major axis and point of interest
Q	Free-surface correction factor
σ_{ut}	Tensile strength
σ_{ys}	Yield strength
E	Young's modulus
v	Poisons ratio
f	Frequency of loading

CHAPTER 1

INTROUCTION

1.1 Introduction

Aluminum and its alloys are being used successfully in a wide range of applications, from packaging to aerospace industries. Due to their good mechanical properties and low densities, these alloys have an edge over other conventional structural materials. Aluminum alloys continue to be the dominating structural materials for aircraft. In most of the aircraft, the air-frame consists of about 80% aluminum by weight. Now-a-days, the cost reduction for aircraft has become an important criterion in many airlines and the selection of material is done on the basis of life cycle approach. The composites are very competitive materials for aircraft structural applications. However, they are generally considered to have higher initial cost, require more manual labour in their production and are more expensive to maintain [1].

In consideration with micro mechanisms based approaches, a large number of investigators held a view that dislocation motion on the preferential planes may be considered as a potential source of crack initiation. Mura and Nakasone [9] proposed a theory to provide *S–N* curve for crack initiation considering yield strength, grain size, dislocation motion, energy dissipation and showed that smaller the grain size, higher is the fatigue stress required for crack initiation. Cheng et al. [7] considered dislocation pile-up to predict the crack initiation life under fretting fatigue loading condition. Lamacq et. al. [12] observed experimentally two crack initiation mechanisms and substantiated by the theoretical explanations. The first mechanism proposes that the crack appears to initiate along a direction ranging from 80˚ to 90˚ with respect to the surface through a brittle tensile fracture mechanism governed by traction stresses and pointed that the initial growth plane depends on the crack location in the contact area. In another mechanism, it is observed that the cracks grow along a direction ranging from 25˚ to 35˚ with respect to the surface through reverse slip mechanism. The sliding originates as a result of dislocation movements along the preferred persistent slip bands which are due to the action of alternative reverse slip and traction–compression on the initiation plane. Resulting from this cyclic sliding, a process of extrusion and intrusion along slip bands is predicted. This mechanism is governed by shear stresses acting on dislocation layers that will lead to the formation of a crack [2].

Previous works has shown that pitting and exfoliation corrosion are particularly deleterious to aircraft structural integrity. In addition to reducing fatigue endurance, pitting also increases the surface area of the component over which fatigue failures can occur [13-15].

Damage by corrosion fatigue is probably the main structural damage factor that affects the performance and the life of aeroplanes and other aluminum alloy structures. However the severity of the degradation of component by corrosion fatigue depends on its location in the structure. Wings of an aircraft are subjected to ground cycles due to the landing and takeoff and to fatigue cycles during the flight, due to atmospheric perturbations and to plane maneuvers. On the contrary of the fuselage, the combination of a flight and a ground cycle corresponds to one single fatigue cycle.

When corrosion takes place at the same time as fatigue, a synergistic effect is developed between the two degradation processes. Damage is enhanced. Corrosion fatigue is a serious issue for airplanes that are exposed to marine and/or polluted air. This environment is particularly detrimental to the corrosion fatigue performance of airplanes since chloride compounds induce the breakdown of the passive film which covers aluminum alloys and which protects them from the atmosphere.

1.2 Microscopic stages of fatigue crack growth [5]

On application of cyclic loading the dislocations and irregularities that were present in the component will increase their severities in the vicinity of nucleated crack which finally leads to the formation of a dominant crack. The crack propagation due to the application of cyclic loading can be divided into two stages as shown in fig 1.1. In ductile solids, cyclic crack growth is envisioned as a process of intense localized deformation in macroscopic slip bands near crack tip.

Stage I fatigue crack growth

The zigzag crack path that has been formed due to single shear of slip planes is termed as stage I crack propagation. In ductile solids, cyclic crack growth can be visualized as a process of intense localized deformation which tends to creation of newer crack surfaces. The direction of propagation of crack will be approximately 45^0 to the direction of load application. It will propagate for two to three grain boundaries.

Stage II fatigue crack growth

As crack propagates the crack tip compromises of many grains. Because of this simultaneous slip planes will develop which will lead to *stage II* crack propagation. In single crystals the transformation of *stage I* to *stage II* causes to the formation of dislocation cell structures and the breakdown of PSB's at the crack tip. During *stage II* crack propagation the direction of crack growth will be almost perpendicular to the direction of application of load. The fracture surfaces created by stage II crack propagation is generally characterized by striations. For certain values of imposed cyclic loads in Paris regime of fatigue crack advance, it has been found that the spacing between adjacent striations correlates with experimentally measured average crack growth rate.

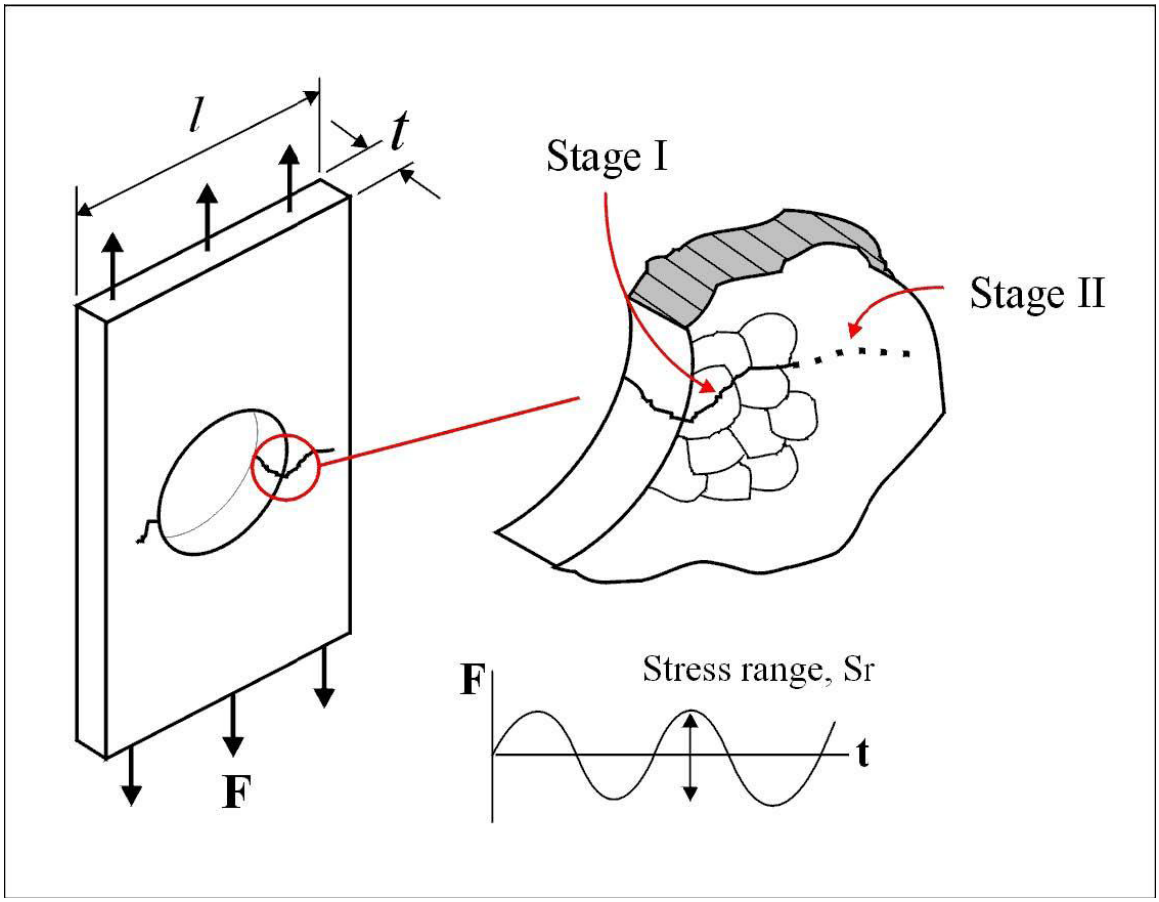

Fig 1.1 Microscopic stages of crack growth

1.3 Environmental effect on crack initiation: Surface roughening and fatigue crack initiation can occur in pure materials in vacuum and at temperatures down to 4.2 K. However the fraction of fatigue life at which crack nucleation occurs can be significantly affected by the test environment. There is a wealth of experimental evidence indicating that the environment plays an important role in dictating the extent of slip irreversibility and fatigue life. Fatigue life is markedly improved in vacuum or in dry, oxygen free media as compared to moist laboratory air [5].

Consider a case of fatigue in pure metals in vacuum or in inert environment. Here, single slip during the tensile loading cycle produce slip steps at the surface. The extent of the surface slip offset can be drastically diminished by reverse slip during the unloading or subsequent compression loading in fully reversed fatigue. In inert environment, surface roughening during fatigue occurs primarily by a random process. On the other hand, when slip steps from during the tensile portion of a fatigue cycle in laboratory air or in a chemically aggressive medium, the chemisorbtion of the embrittling species (such as oxygen or hydrogen) or the formation of oxide layer on the freshly form slip step makes reverse slip difficult on the same slip plane upon load reversal. In the embrittling medium, this process can provide a mechanism of enhanced surface roughening as well as an easier transport of the embrittling species to the bulk of the material preferentially along the persistent slip bands, thereby facilitating crack nucleation.

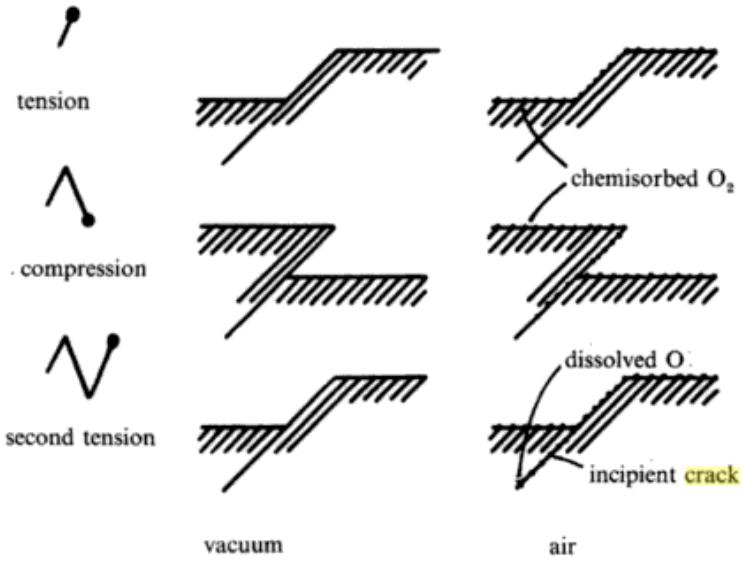

Fig 1.2 A model for fatigue crack nucleation near a free surface by synergistic effect of single slip and environment interaction [5]

1.4 Pre-corrosion importance:

The aim of this project is to study the effect of pre-corrosion on the fatigue life and crack initiation mechanism in 7020-Al alloy. The experiment is practically very much applicable to structures working in aggressive environment. As the corrosion is slow process it can be assumed to have negligible effect on crack propagation and crack initiation constitutes the major part of fatigue life [5], our experimental model to study the fatigue life of pre-corroded structures resembles the actual case upto a reasonable accuracy. Due to localized electrochemical reaction corrosion pits usually form on the metal surface. These corrosion pits formation may take place during their non-operational condition e.g. a fighter plane in its hangar. The fatigue crack propagation occurs during their fight. In those conditions the effect of environment may not be so severe due to short exposure time and high altitude. The crack propagation may be considered in normal non-aggressive atmosphere.

The major alloying elements in 7XXX systems are copper, magnesium, and silicon. These alloys are also subjected to age hardening for strengthening. The microstructure of these alloys consists of precipitates(S-phase Al_2CuMg, η -phase $MgZn_2$, T-phase $Al_2Mg_3Zn_3$, θ-phase Al_2Cu, Z-phase Mg_2Zn_{11}) in a matrix of α solid solution of alloying elements (Zn, Mg, Cu, Mn, Fe, Si) in Al.[10]These precipitates mainly S, η, T phases are responsible for the strengthening of the material. However they frequently reduce localized corrosion resistance, in particular, pitting and exfoliation corrosion. Stronger localized attack on alloys in comparison with aluminum has been ascribed to alloy surface microstructural heterogeneity. Precipitates presence, inclusions and intermetallic particles provoke discontinuities during the layer growth and promote galvanic couples formation with the alloy matrix. Ternary and quaternary Al-based particles frequently found in these alloys exhibit different electrochemical characteristics compared to the surrounding microstructure. Mg-containing particles tend to be anodic, while Cu, Fe and Mn-containing ones tend to be cathodic in relation to the matrix. In both cases, localized dissolution processes are promoted. Since 7XXX aluminum alloys use to have good mechanical performance as aeronautical materials, it is essential to improve localized corrosion processes understanding [4].

1.5 Cyclic Potentiodynamic Polarization Scan technique [11]

The cyclic potentiodynamic polarization technique for corrosion studies is an electrochemical technique that was introduced in the 1960's and refined especially during the 1970's into the fairly simple, routine technique it is today. This technique is especially suited for screening alloys in terms of their risk of suffering localized corrosion in the form of pitting corrosion or crevice corrosion. While cyclic potentiodynamic polarization scans are fairly easy to generate, their interpretation can be far more complex.

The technique is built on the concept that predictions of behavior of a material in an environment can be made by forcing the material from its steady state corrosion rate at a constant voltage scan rate and by observing how the current responds as the voltage force is applied and removed also at a constant voltage scan rate. The material is the alloy under consideration and the environment is that which promotes corrosion. Applied potential is the force. This potential is applied in a controlled manner to an electrode made from the alloy under study.

The potential is ramped at a continuous, often slow rate relative to a reference electrode using an instrument called a potentiostat. Traditionally, the potential is first increased at a constant rate in the anodic or noble direction (forward scan). The scan direction is reversed at some chosen maximum current or voltage and progresses at the same rate in the cathodic or active direction (backward or reverse portion of the scan). The scan is terminated at another chosen voltage, usually either the original corrosion potential or some voltage active with respect to that corrosion potential. The voltage at which the scan is started is usually the corrosion potential as measured after the corrosion reaction has reached steady state. The corrosion behavior is predicted from the structure of the polarization scan.

The electronic device used to generate the cyclic potentiodynamic polarization scan is the potentiostat equipped with the abilities to ramp the applied potential in a controlled manner and then measure the resulting current. Three electrodes are required for the measurement,

(1) The corroding or working electrode made of the material of interest,

(2) The counter electrode made from an inert material such as graphite or platinum, and

(3) A stable reference electrode, some commonly used are,

(a)Hg_2Cl_2 Saturated calomel electrode (SCE) (E=+0.242 V saturated).

(b) Standard hydrogen electrode (SHE) (E=0.000 V)

(c) Silver chloride electrode (E=+0.197 V saturated)

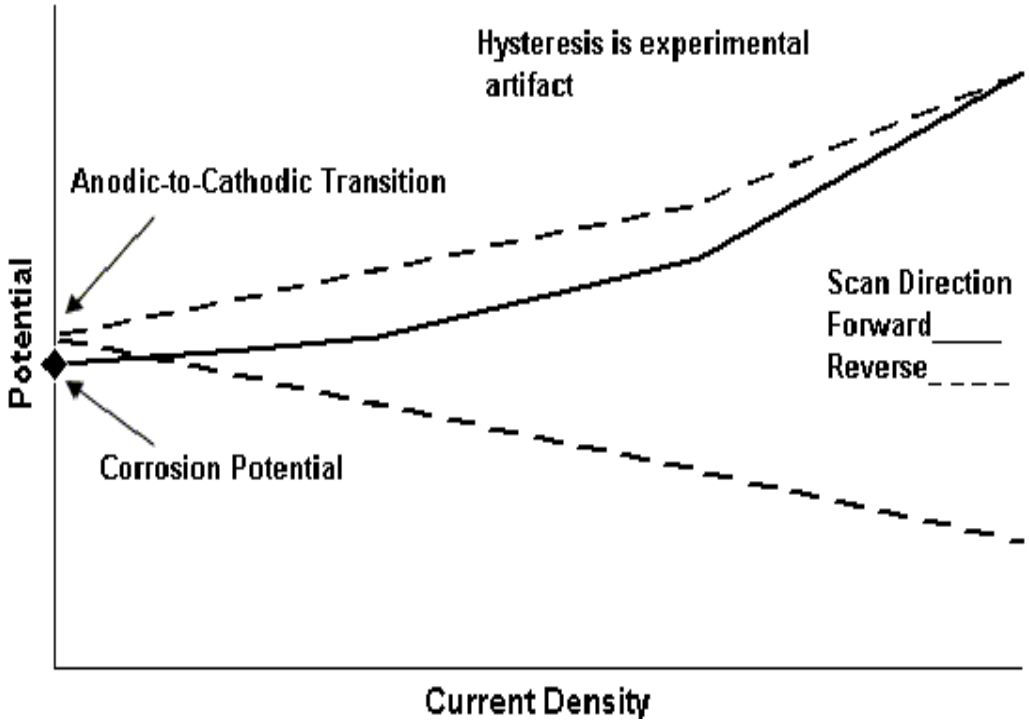

Fig 1.3 Polarization scan for general corrosion

CHAPTER 2

LITERATURE REVIEW

2.1 Metal Fatigue:

Metal fatigue is a phenomenon which results in the sudden fracture of a component after a period of cyclic, fluctuating, alternating or repeated loading. Failure is the end result of a process involving the initiation and growth of a crack, usually at the site of a stress concentration on the surface. Occasionally, a crack may initiate at a fault just below the surface. Eventually the cross sectional area is so reduced that the component ruptures under a normal service load, but one at a level which has been satisfactorily withstood on many previous occasions before the crack propagated. The final fracture may occur in a ductile or brittle mode depending on the characteristics of the material. Fatigue fractures have a characteristic appearance which reflects the initiation site and the progressive development of the crack front, culminating in an area of final overload fracture.

- Initiation site(s).
- Progressive of crack front characterized by beach marks.
- Culminating in an area of final fracture.

Fig.2.1 (a) illustrates fatigue failure in a circular shaft. The initiation site is shown and the shell-like markings, often referred to as beach markings because of their resemblance to the ridges left in the sand by retreating waves, are caused by arrests in the crack front as it propagates through the section. The hatched region on the opposite side to the initiation site is the final region of ductile fracture. Sometimes there may be more than one initiation point and two or more cracks propagate. This produces features as in Fig. 2.1(b) with the final area of ductile fracture being a band across the middle. This type of fracture is typical of double bending where a component is cyclically strained in one plane or where a second fatigue crack initiates at the opposite side to a developing crack in a component subject to reverse bending. Some stress-induced fatigue failures may show multiple initiation sites from which separate cracks spread towards a common meeting point within the section.

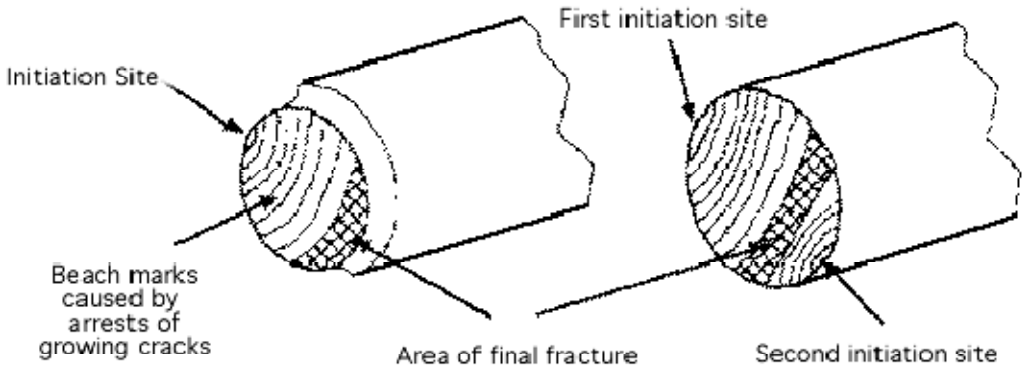

(a) (b)

Fig 2.1 Fatigue failure of circular shaft under bending fatigue stress [8]

2.1.1 Stages of fatigue fracture

The definition above refers to fracture "under repeated or fluctuating stresses having a maximum value less than the tensile strength." (The final fracture may have either brittle or ductile characteristics, depending upon the metal involved and the circumstances of the stress and the environment.) There are three stages of fatigue fracture: initiation, propagation, and final rupture. Indeed, this is the way that most authors refer to fatigue fracture, for it helps to simplify a subject that can become exceedingly complex.

Stage I: Initiation: Initiation is the most complex stage of fatigue fracture and is the stage most rigorously studied by researchers. The most significant factor about the initiation stage of fatigue fracture is that the irreversible changes in the metal are caused by repetitive shear stresses. The accumulation of micro changes over a large number of load applications, called "cumulative damage," has been the subject of study over the years." (Obviously, if this stage can be prevented, there can be no fatigue fracture.) The initiation site of a given fatigue fracture is very small, never extending for more than two to five grains around the origin. At the location of a severe stress concentration, the number depends on the geometry of the part as well as on environmental, stress, metallurgical, and strength conditions, as will become apparent.

Stage II: Propagation: The propagation stage of fatigue causes the micro-crack to change direction and grow perpendicular to the tensile stress. The second, or propagation, stage of fatigue is usually the most readily identifiable area of a fatigue fracture.

Stage III: Final Rupture: As the propagation of the fatigue crack continues, gradually reducing the cross-sectional area of the part or test specimen, it eventually weakens the part so greatly that final, complete fracture can occur with only one more load application. The fracture mode may be either ductile (with a dimpled fracture surface) or brittle (with a cleavage, or perhaps even intergranular, fracture surface) or any combination thereof, depending upon the metal concerned, the stress level, the environment, etc. Stage III represents the "last straw" that broke the camel's back, to borrow a metaphor.

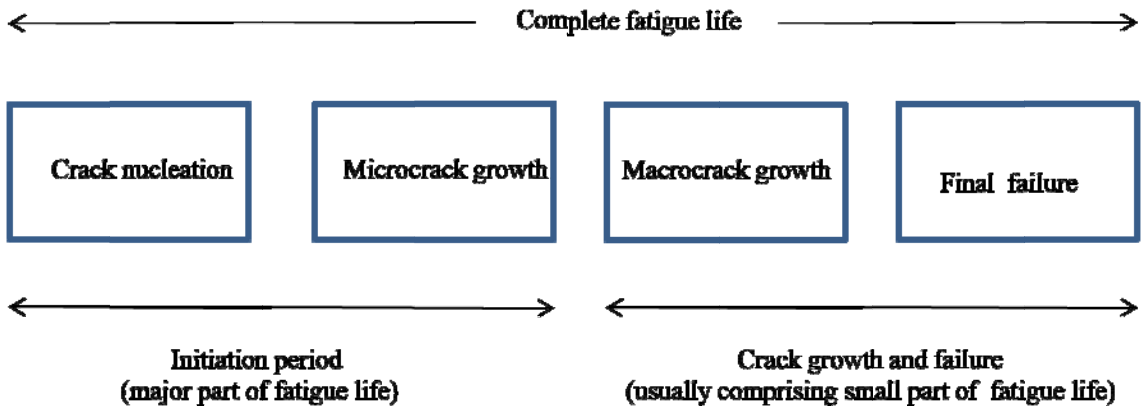

Fig 2.2 Visualization of total fatigue life

2.2 Corrosion problems in Aluminum structural parts:

Corrosion fatigue is serious issue for airplanes and other structures that are exposed to marine and/or polluted environment. This environment is particularly detrimental to the corrosion fatigue performance of airplanes since chloride compounds induce the breakdown of the passive film which covers aluminum alloys and which protects them from the atmosphere. Pits almost always initiate at some chemical or physical heterogeneity at the surface, such as inclusions, second-phase particles, flaws, mechanical damage, or dislocations. The aluminum alloys contain numerous constituent particles, which play an important role in corrosion pit formation.

Because of an aircraft's special service environments, for example, salt water, electrochemical reactions are possible and corrosion pits are readily formed between the constituent particles and the surrounding matrix in these alloys**.**

High-strength, precipitation-hardened aluminum alloys, such as 7075, are used extensively in primary wing and fuselage structures in many Navy and commercial aircraft. These commercial-grade alloys contain numerous constituent particles of various sizes, which may have electrochemical potentials different from those of the surrounding matrices. Because of the Navy's special service environments, these aircraft are subjected to prolonged periods of salt water spray and/or salt fog. In the presence of salt water, electrochemical reactions are possible and corrosion pits are readily formed at or around the constituent particles in 2xxx-series and 7xxx-series aluminum alloys [10-25]. Indeed, many such corrosion pits were observed in wing teardown analyses of Navy aircraft. These corrosion pits, once formed, act as stress concentration sites and can facilitate crack initiation under both cyclic and sustained loading [10-15]. However, only limited studies of the effects of pre-existing pits on fatigue crack initiation in aluminum alloys have been performed. Additionally, many of these studies used smooth specimen geometry and results could not be easily translated to more complex aircraft structural configurations, such as rivet holes. Thus, quantitative characterization of the influences of corrosion pits on fatigue crack initiation in 7xxx-series alloys, using a fracture mechanics approach, is highly desirable and is essential for the development of life prediction methodology for aging aircraft.

As shown various investigations, corrosion criticality has implications for the management of the structural integrity of aircraft and other aluminum structures. The spread of fatigue critical regions due to pitting corrosion means that those regions of aircraft, which were considered to be safe by design, may not actually be safe once corroded. There are at least two scenarios to be considered. In the first, the corrosion of low stress regions of a fatigue critical component means that the area of that component requiring inspection will need to be increased if safe operation is to be ensured. This increases the cost of maintenance and, consequently, the cost of fleet operations. The second scenario is where the corrosion of a durability component (i.e. a component that is designed with a fatigue life far in excess of the aircraft) may cause it to fail during the life of the aircraft. Such a failure could prevent the safe operation of the aircraft and may lead to expensive repairs.

2.2.1 **Corrosion of Aluminum and Its Alloys: Forms of Corrosion**

Corrosion is the chemical reaction of a metal, in this case aluminum, with its environment, which leads to the deterioration of the properties of metals, aluminum in this case. Aluminum is a very reactive metal, but it is also a passive metal. This contradictory nature is explainable because nascent aluminum reacts with oxygen or water and forms a coherent surface oxide which impedes further reaction of aluminum with the environment.

Corrosion does take place when this protective layer is either unstable or defective. Corrosion in aluminum alloys takes one of two forms: pitting or intergranular corrosion. Pitting takes place in environments where the protective film is partially stable. In these cases, corrosion usually originates adjacent to flaws in the microstructure of the film and therefore pitting occurs at random points on the exposed aluminum alloy where these defects are present in the oxide film. Intergranular corrosion results in selective corrosion at the grain boundaries, or any precipitate-free zones that might be formed adjacent to them, with the remainder of the matrix undergoing very little corrosion. Intergranular corrosion occurs because of the formation of precipitates along the grain boundaries, which are more anodic with respect to the interior of the grains. As a result, preferential dissolution occurs at these sites where these precipitates, or the precipitate-free zones, undergo anodic reactions. Al 7xxx alloys are generally more resistant to intergranular

corrosion because the Mg and Si precipitates which form at grain boundaries during heat treatment have a similar electrode potential to the matrix [6].

Aluminum alloys may corrode via several different pathways. Recognizing the pathway or the forms of aluminum corrosion is an important step to determine the appropriate remedy for each probe. Some of the common modes of failures in aluminum are:

Atmospheric Corrosion: Atmospheric corrosion is defined as the corrosion or degradation of material exposed to the air and its pollutants rather than immersed in a liquid. This has been identified as one of the oldest forms of corrosion and has been reported to account for more failures in terms of cost and tonnage than any other single environment. Many authors classify atmospheric corrosion under categories of dry, damp, and wet, thus emphasizing the different mechanisms of attack under increasing humidity or moisture.

Corrosivity of the atmosphere to metals varies greatly from one geographic location to another, depending on such weather factors as wind direction, precipitation and temperature changes, amount and type of urban and industrial pollutants, and proximity to natural bodies of water. Service life may also be affected by the design of the structure if weather conditions cause repeated moisture condensation in unsealed crevices or in channels with no provision for drainage.

Uniform Corrosion

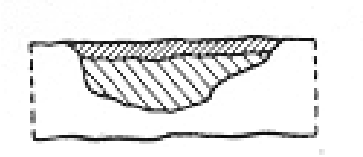

Fig.2.3 Uniform corrosion: The reaction starts at the surface and proceeds uniformly.

General corrosion, or uniform corrosion, occurs in the solutions where pH is either very high or very low, or at high potentials in electrolytes with high chloride concentrations. In acidic (low pH) or alkaline (high pH) solutions, the aluminum oxide is unstable and thus non-protective.

Galvanic Corrosion

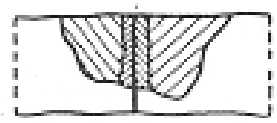

Fig.2.4 Galvanic corrosion: Increased corrosion in crevices or cracks or at contact surfaces between two metal articles.

Economically, galvanic corrosion creates the largest number of corrosion problems for aluminum alloys. Galvanic corrosion, also known as dissimilar metal corrosion, occurs when aluminum is electrically connected to a more noble metal, and both are in contact with the same electrolyte.

Crevice Corrosion:

Crevice corrosion requires the presence of a crevice, a salt water environment, oxygen (Fig. 1). The crevice can result from the overlap of two parts, or gap between a bolt and a structure. When aluminum is wetted with the saltwater and water enters the crevice, little happens initially. Over time, inside the crevice oxygen is consumed due to the dissolution and precipitation of aluminum.

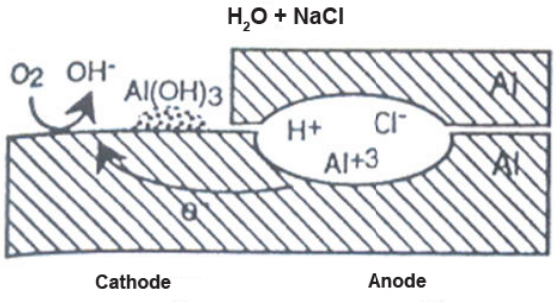

Fig.2.5 Crevice corrosion [6]

Crevice corrosion can occur in a saltwater environment if the crevice becomes deaerated, and the oxygen reduction reaction occurs outside of the crevice mouth. Under these conditions, the crevice becomes more acidic, and corrosion occurs at an increasing rate.

Pitting Corrosion

Fig 2.6 Localized corrosion (pitting corrosion)

The basis metal is eaten away and perforated in places in the manner of holes, the rest of the surface being affected only slightly or not at all.

Fig.2.7 Wide pitting corrosion: The corrosion causes localized scarring.

Corrosion of aluminum in the passive range is localized, usually manifested by random formation of pits. The pitting-potential principle establishes the conditions under which metals in the passive state are subject to corrosion by pitting.

Pitting corrosion is very similar to crevice corrosion. Pitting of aluminum alloys occurs if the electrolyte contains a low level of chloride anions, and if the alloy is at a potential above the "pitting potential." Pitting initiates at defects on the surface of the aluminum, such as at second phase particles or on grain boundaries.

Deposition Corrosion

In designing aluminum and aluminum alloys for satisfactory corrosion resistance, it is important to keep in mind that ions of several metals have reduction potentials that are more cathodic than the solution potential of aluminum and therefore can be reduced to metallic form by aluminum. For each chemical equivalent of so-called heavy-metal ions reduced, a chemical equivalent of

aluminum is oxidized. Reduction of only a small amount of these ions can lead to severe localized corrosion of aluminum, because the metal reduced from them plates onto the aluminum and sets up galvanic cells.

The more important heavy metals are copper, lead, mercury, nickel, and tin. The effects of these metals on aluminum are of greatest concern in acidic solutions; in alkaline solutions, they have much lower solubility and therefore much less severe effects.

Intergranular Corrosion

Fig.2.8 Intergranular corrosion: Imperceptible or barely perceptible from outside, since the corrosion proceeds at the grain boundaries.

Intergranular (intercrystalline) corrosion is selective attack of grain boundaries or closely adjacent regions without appreciable attack of the grains themselves. Intergranular corrosion is a generic term that includes several variations associated with different metallic structures and thermomechanical treatments. Intergranular corrosion is caused by potential differences between the grain-boundary region and the adjacent grain bodies.

The location of the anodic path varies with the different alloy systems. In 2xxx series alloys, it is a narrow band on either side of the boundary that is depleted in copper; in 5xxx series alloys, it is the anodic constituent Mg_2Al_3 when that constituent forms a continuous path (corrosion channel) along a grain boundary; in copper-free 7xxx series alloys, it is generally considered to be the anodic zinc- and magnesium-bearing constituents on the grain boundary. The 6xxx series alloys generally resist this type of corrosion, although slight intergranular attack has been observed in aggressive environments.

Exfoliation Corrosion

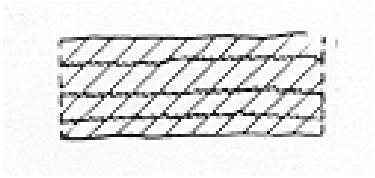

Fig.2.9 Exfoliation corrosion: Occurs in deformed articles. Corrosion follows "fiber orientation".

Exfoliation corrosion is a special form of intergranular corrosion which occurs when the grains are flattened by heavy deformation during hot or cold rolling, and where no recrystallization has occurred. Exfoliation is characteristic for the 2000 (Al-Cu), 5000 (Al-Mg), and 7000 (Al-Zn-Mg) series alloys which have grain boundary precipitation or depleted grain boundary regions.The remedy for exfoliation is similar to above for IG corrosion. To prevent the exfoliation of alloy 7075-T6, the newer alloy 7150-T77 can be substituted wherever 7075-T6 is used.

Erosion-Corrosion

Erosion-corrosion of aluminum occurs in high velocity water and is similar to jet-impingement corrosion. Erosion-corrosion of aluminum is very slow in pure water, but is accelerated at pH > 9, especially with high carbonate and high silica content of the water.

Aluminum is very stable is neutral water; however it will corrode in either acidic or alkaline waters. To prevent erosion-corrosion, one may change the water chemistry or reduce the velocity of the water, or both. For the water chemistry, the pH must be below 9, and the carbonate and the silica levels must be reduced.

Stress Corrosion Cracking (SCC)

Stress corrosion cracking (SCC) is the bane of aluminum alloys. SCC requires three simultaneous conditions, first a susceptible alloy, second a humid or water environment, and third a tensile stress which will open the crack and enable crack propagation. SCC can occur in two modes, intergranular stress corrosion cracking (IGSCC) which is the more common form, or transgranular SCC (TGSCC). In IGSCC, the crack follows the grain boundaries. In transgranular stress corrosion cracking (TGSCC), the cracks cut through the grains and are oblivious to the grain boundaries.

The general trend to use higher strength alloys peaked in 1950 with alloy 7178-T651 used on the Boeing 707, then the industry changed to using lower strength alloys. The yield strength of the upper wing skin did not exceed the 1950 level until the Boeing 777 in the 1990s. The reason lower strength alloys were selected for the Boeing 747 and the L-1011 was that the aircraft designers chose an alloy with better SCC resistance rather than the higher yield strength.

Corrosion Fatigue

Corrosion fatigue can occur when an aluminum structure is repeatedly stressed at low stress levels in a corrosive environment. A fatigue crack can initiate and propagate under the influence of the crack-opening stress and the environment. Similar striations may sometimes be found on corrosion fatigued samples, but often the subsequent crevice corrosion in the narrow fatigue crack dissolves them.

Fatigue strengths of aluminum alloys are lower in such corrosive environments as seawater and other salt solutions than in air, especially when evaluated by low-stress long-duration tests. Like SCC of aluminum alloys, corrosion fatigue requires the presence of water. In contrast to SCC, however, corrosion fatigue is not appreciably affected by test direction, because the fracture that results from this type of attack is predominantly transgranular.

Filiform Corrosion

Filiform corrosion (also known as wormtrack corrosion) is a cosmetic problem for painted aluminum. Pinholes or defects in the paint from scratches or stone bruises can be the initiation site where corrosion begins with salt water pitting. Filiform corrosion requires chlorides for initiation and both high humidity and chlorides for the propagation of the track.

The propagation depends on where and how the alloy is used. The filament must be initiated by chlorides, and then it proceeds by a mechanism similar to crevice corrosion. The head is acidic, high in chlorides, and deaerated and is the anodic site. Oxygen and water vapor diffuse through the filiform tail, and drive the cathodic reaction. Filiform corrosion can be prevented by sealing defects with paint or wax, and keeping the relative humidity low.

Microbiological Induced Corrosion

Microbiological Induced Corrosion (MIC) applies to a corrosive situation which is caused or aggravated by the biological organisms. A classic case of MIC is the growth of fungus at the water/fuel interface in aluminum aircraft fuel tanks. The fungus consumes the high octane fuel, and excretes an acid which attacks and pits the aluminum fuel tank and causes leaking. The solution for this problem is to control the fuel quality and prevent water from entering or remaining in the fuel tanks. If fuel quality control is not feasible, then fungicides are sometimes added to the aircraft fuel.

2.3 Potentiostat and forced corrosion [11]:

Potentiostats are amplifiers used to control a voltage between two electrodes, a working electrode and a reference electrode, to a constant value.

To achieve this, some conditions have to be matched: Reference electrodes are electrodes, which maintain a constant voltage referred to the potential of the hydrogen electrode (which is by convention established as the potential reference point). A silver wire, covered with a silver chloride layer, dipping in a chloride solution, or calomel Hg_2Cl_2 is a simple reference electrode. However, as soon as a current passes this electrode, it is polarized, that means its potential varies with the current. Hence, to maintain a stable potential, no current is allowed to pass the reference electrode. Imagine that any amplifier input has a limited input resistance, and a small current passes this input. A potentiostat must have a very high input resistance to meet this condition, in the range of Gigaohms to Teraohms or even higher.

We are forced to introduce a third electrode, which we call counter electrode. A current is forced between working electrode and counter electrode, high enough and in proper polarity to keep the working electrode potential at a constant value with respect to the reference electrode.

The potentiostat has two tasks: To measure the potential difference between working electrode and reference electrode without polarizing the reference electrode, and to compare the potential difference to a preset voltage and force a current through the counter electrode towards the working electrode in order to counteract the difference between preset voltage and existing working electrode potential.

Experimental variables affecting corrosion rate [36-40]:

1. Corrosion Potential
2. Solution Resistance
3. Scan Rate i.e. the rate at which the potential is ramped
4. Point of Scan Reversal

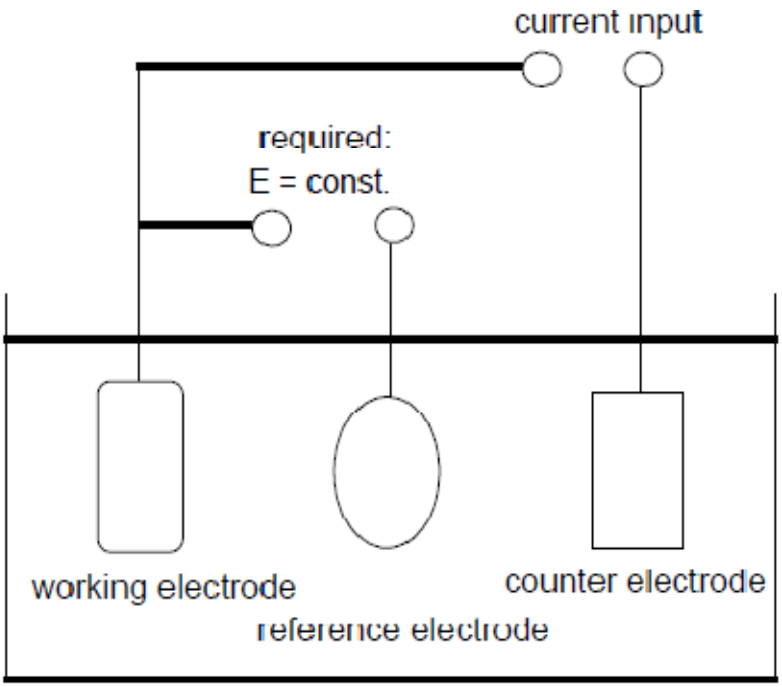

Fig.2.10 Principle of a potential-controllable electrochemical cell[11]
(potentiostat/ galvanostat)

Three electrodes are required for the measurement,

1) The corroding or working electrode made of the material of interest: The working electrode is the electrode in an electrochemical system on which the reaction of interest is occurring.
2) The counter electrode made from an inert material such as graphite or platinum: The counter electrode, also known as the auxiliary or second electrode, can be any material which conducts easily and won't react with the bulk solution. Reactions occurring at the counter electrode surface are unimportant as long as it continues to conduct current well. To maintain the observed current the counter electrode will often oxidize or reduce the solvent or bulk electrolyte.
3) A stable reference electrode: A Reference electrode is an electrode which has a stable and well-known electrode potential. Some commonly used are,

   (a)Hg_2Cl_2 Saturated calomel electrode (SCE) (E=+0.242 V saturated).

   (b) Standard hydrogen electrode (SHE) (E=0.000 V)

   (c) Silver chloride electrode (E=+0.197 V saturated)

2.3.1 Cyclic Potentiodynamic Polarization Scan (technique for forced corrosion):

Cyclic voltammetry as it is also known is built on the concept that predictions of behavior of a material in an environment can be made by forcing the material from its steady state and observing how it responds as the force is removed at a constant rate and the material is relaxed back to its steady state condition. In this case, the material is an alloy and the environment promotes electrochemical corrosion. Applied potential is the force. This potential is applied in a controlled manner to an electrode made from the alloy under study. The potential is ramped at a continuous, often slow rate (scan rate) relative to a reference electrode using an instrument called a potentiostat Fig 2.11.

Potentiostat is an electronic instrument that automatically maintains an electrode at a constant or controlled voltage relative to a suitable reference electrode in a medium containing enough ionic character to carry a current.

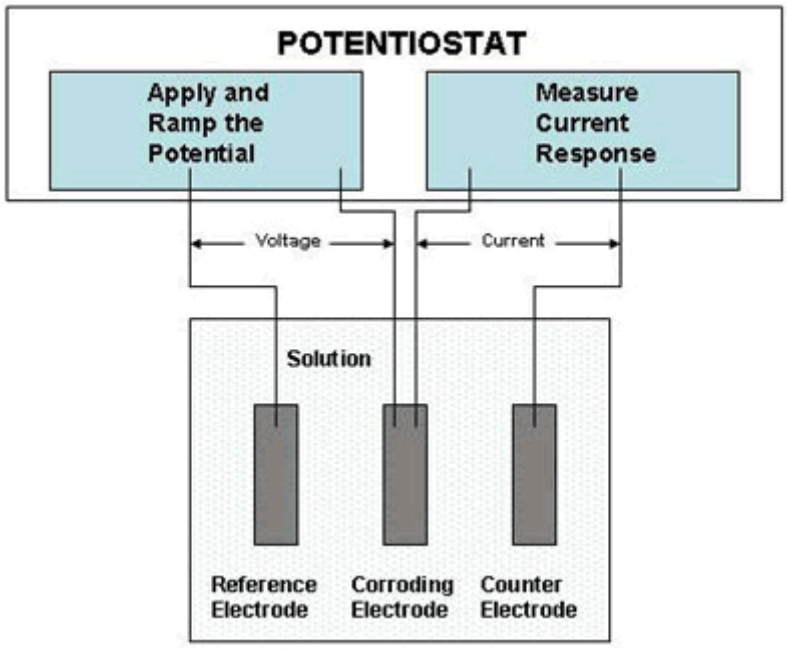

Fig 2.11 Schematic diagram of potentiostat [11]

Traditionally, the potential is first increased at a constant rate in the anodic or noble direction (forward scan). The scan direction is reversed at some chosen maximum current or voltage and progresses at the same rate in the cathodic or active direction (backward or reverse portion of the scan). The scan is terminated at another chosen voltage, usually either the original corrosion

potential or some voltage active with respect to that corrosion potential. The voltage at which the scan is started is usually the corrosion potential.

Cyclic voltammetry or CV is a type of potentiodynamic electrochemical measurement. The method uses a reference electrode, working electrode, and counter electrode which in combination are referred to as a three-electrode setup. Electrolyte is usually added to the test solution to ensure sufficient conductivity. The combination of the solvent, electrolyte and specific working electrode material determines the range of the potential.

In cyclic voltammetry, the electrode potential ramps linearly versus time as shown. This ramping is known as the experiment's scan rate (V/s). The potential is measured between the reference electrode and the working electrode and the current is measured between the working electrode and the counter electrode. This data is then plotted as current (i) vs. potential (E). As the waveform shows, the forward scan produces a current peak for any analytes that can be reduced (or oxidized depending on the initial scan direction) through the range of the potential scanned. The current will increase as the potential reaches the reduction potential of the analyte, but then falls off as the concentration of the analyte is depleted close to the electrode surface. If the redox couple is reversible then when the applied potential is reversed, it will reach the potential that will reoxidize the product formed in the first reduction reaction, and produce a current of reverse polarity from the forward scan. This oxidation peak will usually have a similar shape to the reduction peak. As a result, information about the redox potential and electrochemical reaction rates of the compounds are obtained.

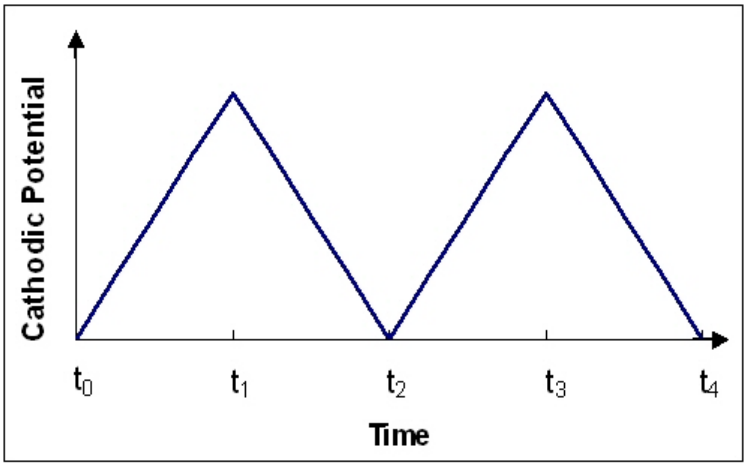

Fig 2.12 Cyclic voltametry potential waveform [42]

2.3.2 Pitting Potential:

The pitting potential is a phenomenological potential at which the forward or ascending portion of the cyclic potentiodynamic polarization scan suddenly changes from a relatively slow rise in current with respect to voltage to a very rapid rise in current with respect to voltage. Very often the slope ($\Delta(\log I)/\Delta E$) even approaches infinity above the pitting potential as shown in the polarization scan depicting localized corrosion. The current tends to be greater on the reverse scan than on the forward scan at the same potential giving rise to the so-called negative hysteresis. This potential is not a function of the alloy alone. It tends to be a function also of the scan rate, environment, surface finish, current and potential at which the scan direction was reversed, and impurities in the surface of the alloy. When the experiment is over, the electrode itself will often show small pits. The value suggested for this input is the difference between the potential at which the slope (Δ (log (I)/ΔE) becomes large as shown on the figure corresponding to localized corrosion and the corrosion potential. If the pitting potential occurs at less than 0.1 $\mu A/cm^2$ (10^{-7} A/cm^2), the potential should be read at 0.1 $\mu A/cm^2$ ($10^{-7} A/cm^2$). This suggestion arises from the original training that included potentiodynamic polarization scans generated on a number of different instruments, some of which were set so the lowest current reading was 10^{-7} amp/cm^2. Though this lowest current designation is somewhat arbitrary, consistency is guaranteed as long as this voltage, the repassivation voltage, and the anodic-to-cathodic transition are read at the same current density value between about 10^{-8} amp/cm^2 and 10^{-7} amp/cm^2. The corrosion potentials for the systems used in training were the open circuit potentials measured after at least 18 hours of exposure to get as close as possible to steady state. A corrosion potential measured after such extended immersion should be used.

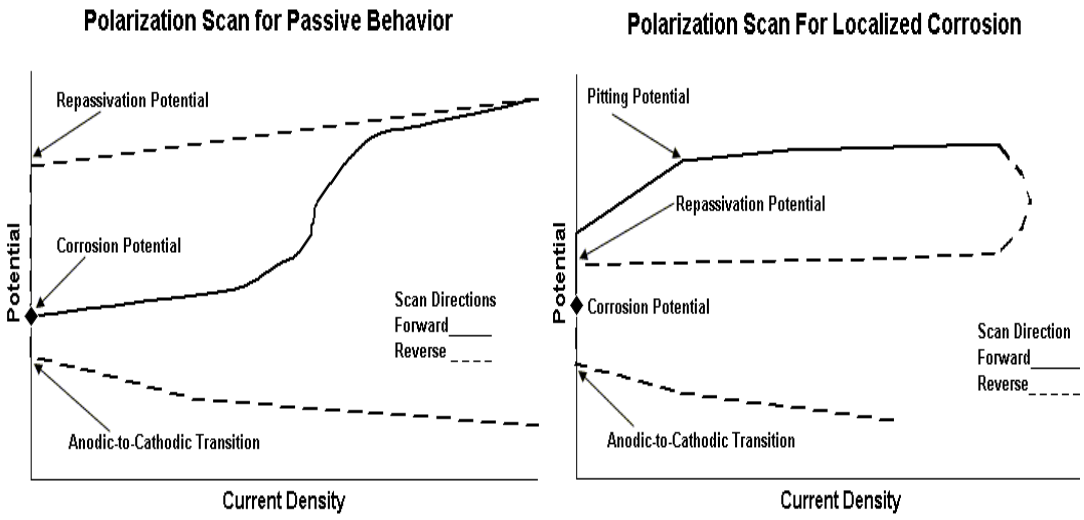

Fig 2.13 Polarisation scan for (i)passivation and(ii) pitting corrosion[11]

As shown on the figure corresponding to localized corrosion, the change in slope is fairly sharp so the pitting potential should be fairly easy to pinpoint. The current will increase very rapidly with small changes in potential. This behavior cannot be confused with behavior in which there is a gentle change in slope of the potential versus log (current density) curve. That type of change could signal the transpassive region. If the polarization scan is not pushed too far into that region, upon reversing the direction of the polarization scan at any potential the current can often be less than that on the forward portion of the scan giving rise to the so-called positive hysteresis between the two portions of the scan. In this case, no pitting is observed and a value of 10 is entered for the pitting potential. The polarization scan depicting passive behavior is an example of this type of behavior.

2.4 The Equivalent Crack Size (ECS) approach:

The ECS approach is a potential method by which pitting corrosion can be treated as a fatigue crack, assuming it is no longer growing due to corrosion. The ECS concept is a modification of the EIFS (equivalent initial flaw size) concept which was originally suggested by Rudd and Gray [26] as a means of estimating the effect of initial surface state on fatigue life. If successful in predicting the effects of corrosion, the ECS approach could allow corrosion pits to be evaluated using the same criteria used for fatigue cracks. Maintenance actions could then be scheduled more economically than using the 'find and fix' policy. If it could be shown that pitting corrosion was not going to cause an unacceptable loss of structural integrity prior to the next depot maintenance then the removal of the corrosion could be delayed to that time. This would reduce maintenance costs and increase aircraft availability. The underlying assumption of the ECS approach is that a pit of a certain size will act like a crack of a related size [12,28]. Given accurate fatigue crack growth (FCG) data, the fatigue crack initiated from the pit will grow in an identical manner and at the same rate as that from the 'equivalent crack' after an initial stage during which the fatigue crack from the pit is established.

Damage due to pitting and inter granular corrosion is simulated by a surface crack which comprehends the total corrosion damaged area Fig 2.14(a). The definitive model surface crack has the dimension of the deepest (a) and widest (2c) corrosion damages Fig 2.14(b). The definitive model surface crack has the dimension of the deepest (a) and widest (2c) corrosion damages also in the case of coalescence of several pits as Fig 2.14(c).

Fig 2.15 illustrates the parameters that can be used to characterize a pit's size. These include:

- Pit cross-sectional area
- Maximum pit depth
- Maximum pit width
- Pit surface opening width
- Local pit radius
- Pit aspect ratio = ½(maximum pit width)/(maximum pit depth)

It should be noted, however, that some of the above quantities cannot be measured in-service. More likely metrics for in-service use include maximum pit depth, maximum pit width and pit opening width. As can be seen in Fig 2.15 the maximum depth of a pit can exceed its apparent depth due to the complex shape of the pit. Corrosion pits in aluminium alloys tend to be very convoluted in shape making it very difficult to examine them in-service. Furthermore, corrosion pits in aluminum alloys are commonly full of corrosion product [27].

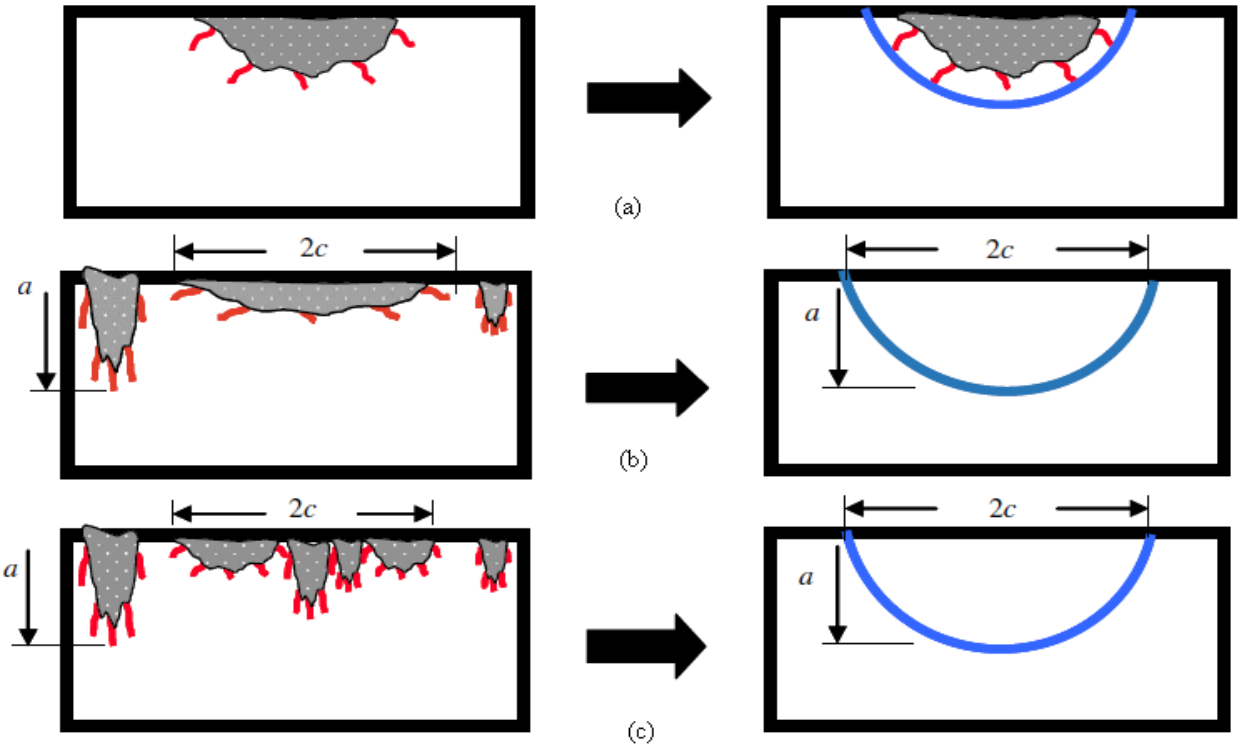

Fig 2.14 Equivalent elliptical model for channeled pits [39]

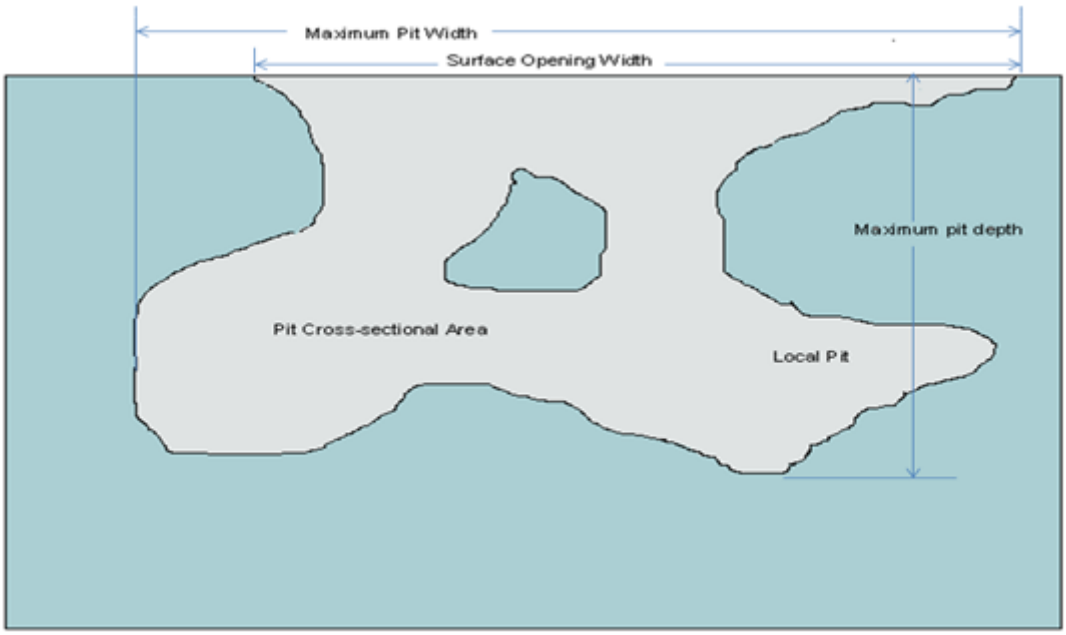

Fig 2.15 Various measures of pit size for use as pit metrics [27]

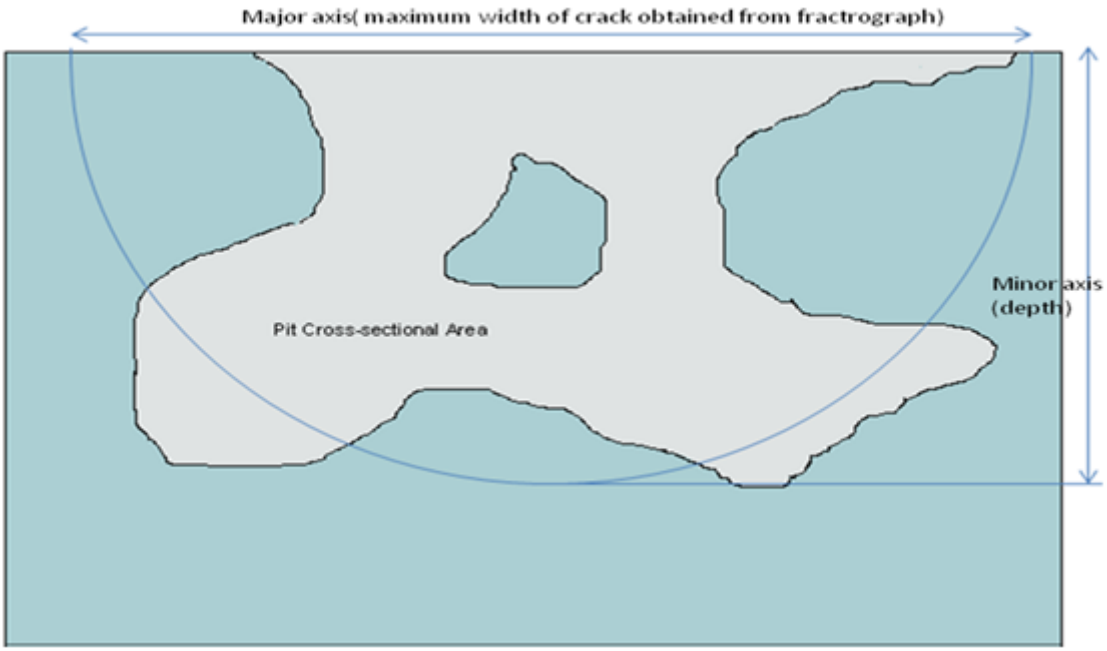

Fig 2.16 Equivalent elliptical crack used in model

2.5 Stress concentration based on linear elasticity (for elliptical hole):

The corrosion pits formed on the metal surface are usually semi-elliptical in shape. Therefore an attempted has been made to understand the effect of elliptical and semi-elliptical crack on SIF. Consider an elliptical hole in a two-dimensional infinite solid under remote uniaxial tension. The major and minor axes for the elliptical hole are denoted as c and b, as shown in Fig 2.17.

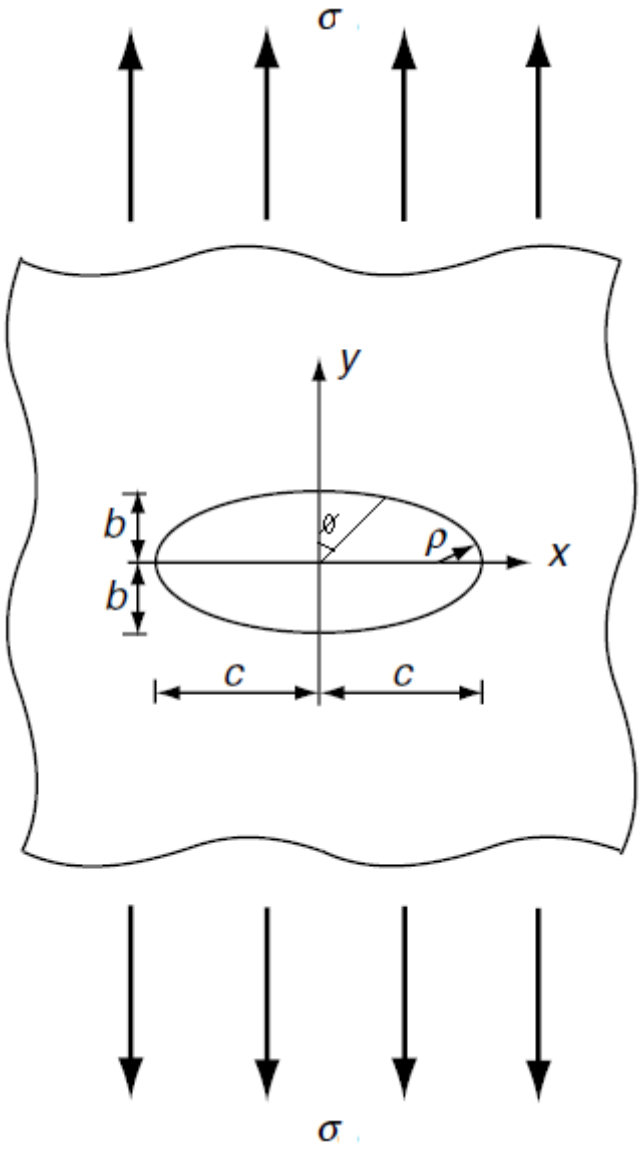

Fig 2.17 An elliptical hole in a two-dimensional infinite solid under remote tension σ.

The elliptical hole surface can be described by the equation

$$\frac{x^2}{c^2}+\frac{y^2}{b^2}=1 \qquad (2.1)$$

The radius of curvature at $x = \pm c$ and $y = \pm \infty$ is denoted as ρ, as shown in the figure. The radius of curvature ρ can be related to c and b as

$$\rho = \frac{b^2}{c} \qquad (2.2)$$

The two-dimensional infinite solid is subjected to a uniformly normal stress σ_∞ in the y direction at $y = \pm \infty$. The linear elasticity solution gives the stress solution at $x = \pm c$ and $y=0$ as

$$\sigma_{yy}(x = \pm c, y = 0) = \sigma\left(1 + \frac{2c}{b}\right) \qquad (2.3)$$

Based on Equation (2.2), Equation (2.3) can be rewritten as

$$\sigma_{yy}(x = \pm c, y = 0) = \sigma\left(1 + 2\sqrt{\frac{c}{\rho}}\right) \qquad (2.4)$$

We can define the stress concentration factor K_t for the elliptical hole under the remote uniaxial tension as

$$K_t = \frac{\sigma_{yy}(x = \pm c, y = 0)}{\sigma} = \left(1 + 2\sqrt{\frac{c}{\rho}}\right) \qquad (2.5)$$

2.6 Stress intensity factors of large plates with elliptical and semi elliptical cracks:[5]

Consider a plate specimen containing an elliptical crack. Let the major and minor axes of the ellipse be *2c* and *2b* as shown in figure. The stress intensity for the embedded elliptical flaw varies along the crack front as a function of the angle *ø* see figure. When the dimensions of the cracked body are much larger than *b* and *c*

$$K_{\mathrm{I}} = \frac{\sigma\sqrt{\pi b}}{\Psi}\left(\sin^2\phi + \frac{b^2}{c^2}\cos^2\phi\right)^{1/4} \qquad (2.6)$$

Where Ψ is elliptical integral of the second kind, which is given by

$$\Psi = \int_0^{\pi/2}\left\{1 - \left(1 - \frac{b^2}{c^2}\right)\sin^2\phi\right\}^{1/2} d\phi \qquad (2.7)$$

K_I is maximum when ϕ=90°. Using a series for Ψ, it can be shown that

$$\Psi = \frac{3\pi}{8} + \frac{\pi}{8}\left(\frac{b^2}{c^2}\right) \qquad (2.8)$$

For the case of semi-elliptical surface cracks,

$$K_I = \frac{1.12\sigma\sqrt{\pi b}}{\sqrt{Q}} \qquad (2.9)$$

Where, the multiplier 1.12 is the free-surface correction factor, Q is the flaw shape parameter extracted from Ψ in the equation (2.7). $Q = \Psi^2$ in the elastic limit, $\sigma/\sigma_y \rightarrow 0$, where, σ is the applied stress and σ_y is the yield stress of the material. Additional corrections may have to be made to equation (2.9) to account for proximity of the free surface to the crack front (depending on the relative magnitudes of b and the specimen thickness) and for crack-tip plasticity. The modified value of Q incorporating the plasticity correction is usually taken to be

$$Q \approx \Psi - 0.212(\sigma^2/\sigma_y^2) \qquad (2.10)$$

Finally the equation (2.6) reduces to:

$$K_I = \frac{1.12\sigma\sqrt{\pi b}}{\frac{3\pi}{8} + \frac{\pi}{8}\left(\frac{b}{c}\right)^2} \qquad (2.11)$$

CHAPTER 3

OBJECTIVE OF INVESTIGATION

Objective:

Corrosion fatigue is serious issue for structures and machine components exposed to marine and/or polluted environment. Saline environment is particularly detrimental to the fatigue performance of aluminum alloys. This is due to breakdown of the passive film which covers the alloys and protects them from the atmosphere. Surface pits are common sits for initiation of fatigue cracks. Pits usually occur at the sites of some chemical or physical heterogeneity at the surface such as inclusions, second-phase particles, flaws, mechanical damage etc. The structural aluminum alloys contain numerous constituent particles and are responsible for surface pits formation and subsequent crack initiation.

Aluminum alloys are usually subjected to saline atmosphere during cycles. Marine atmosphere is very common corrodent for Al-alloy structures. This environment is particularly detrimental due to localized electrochemical reaction corrosion pits formation on the metal surface. This corrosion pits formation may take place during their non-operational condition e.g., a fighter plane in its hangar. The fatigue crack propagation occurs during their fight. In those conditions the effect of environment may not be so severe due to short exposure time and high altitude. The crack propagation may be considered in normal non aggressive atmosphere. In the present investigation an attempt has been made to investigate the effect of pre-corrosion on the life of 7020 Al alloy. In first set of experimentation, notched specimens are subjected to Moore rotating bending fatigue test. In second set, forced corrosion of samples has been done to accelerate the corrosion and visualize its effect on fatigue life. These forced corroded specimens were subsequently subjected to rotating beam as well as push-pull tests.

CHAPTER 4

EXPERIMENTATION

4.1 Specimen preparation

The material available was in the form of rolled 25 mm thickness 7020 aluminum alloy sheet. This alloy is used in ground transportation systems, such as Armoured vehicles, military bridges, motor cycles, bicycle frames, and aircraft and ship structures. This alloy is usually subjected to very aggressive environmental conditions during its service. The chemical composition of the present alloy is presented in Table 4.1.

Table 4.1: Chemical composition of 7020 Al alloy

Element	Cu	Mg	Mn	Fe	Si	Zn	Al
Wt.%	0.05	1.20	0.43	0.37	0.22	4.60	balance

The sheet was cut into pieces according to the dimension of the standard fatigue test specimen on Moore fatigue testing machine. The dimensional details of specimen are shown in Fig.4.1.

Prior to fabrication, the alloy material in consideration was given T7 heat treatment comprising, solution heat treatment at 520°C followed by quenching and subsequently 2-stage artificial aging at 110°C and 150°C for 10 hours and 20 hours respectively followed by air cooling. This was done in order to maintain the dimensional uniformity, since the heat treatment of the specimen itself after fabrication can distort its shape. The above processes yield a uniform microstructure and improved mechanical properties. The measured average hardness of the specimen after a series of experiment is 133 VHN. The mechanical properties of the alloy are given in Table 4.2. Microstucture of the alloy under investigation is presented in Fig. 4.1[47].

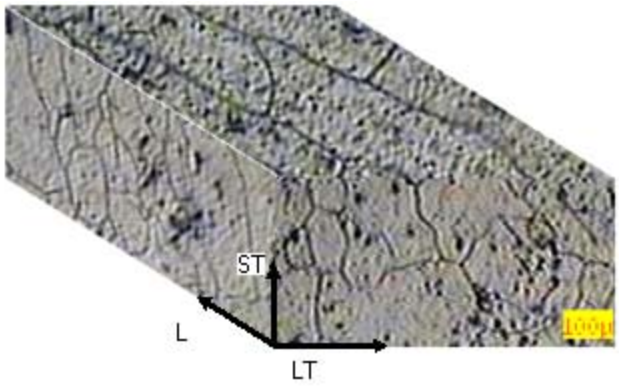

Fig 4.1 Microstructure of the alloy[47]

Table 4.2: Mechanical properties of 7020-T7 Al alloy:

Tensile strength(σ_{ut})	352.14MPa
Yield strength(σ_{ys})	314.7MPa
Young's modulus (E)	70,000MPa
Elongation in 40 mm	21.54%
Poisons ratio(v)	0.33

The fabricated specimens were divided into two lots. In one set of specimens V-notch of 1mm depth of notch tip radius 0.25mm were machined.

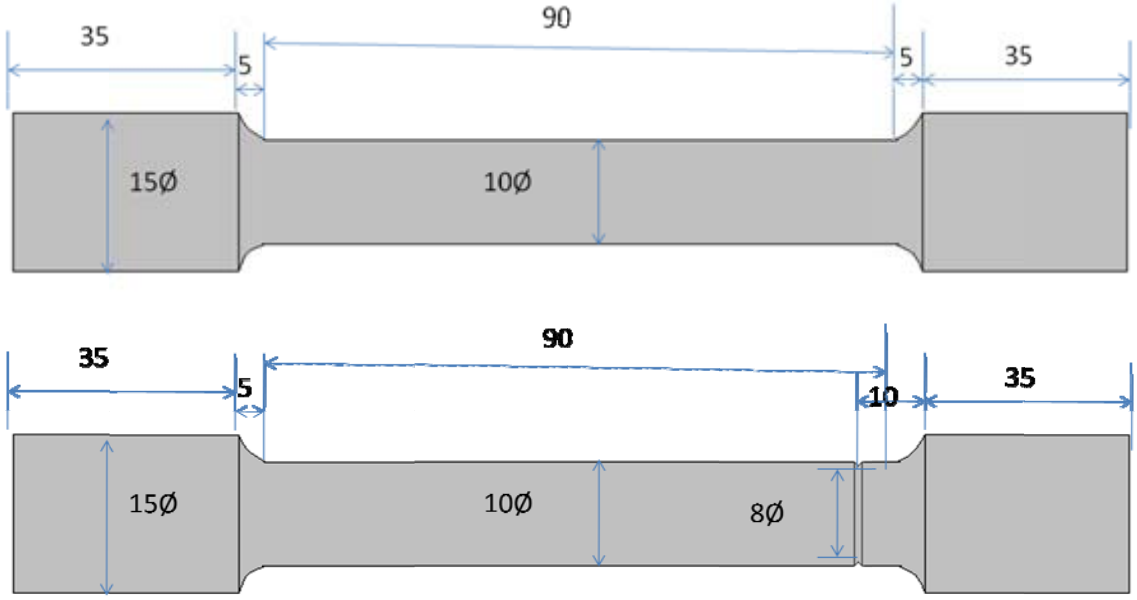

Fig 4.2 Fatigue test specimens

4.2 Corrosion of specimens:

Aqueous solution of sodium chloride was prepared by dissolving 3.5% analytical grade NaCl in distilled water. The pH of the solutions was set to 8.2 for the present investigation. The pre-corrosion of test specimens were conducted in three different conditions. Following are the details of the corrosion schedule:

1. A set of notched specimens were pre-corroded by immersing them in the above prepared solution for 100 h at room temperature (30 ºC). The pH of solution was monitored at regular interval. The solution was replaced at the end of each day, in order to maintain the concentration of the solution.

2. Second batch of specimens, comprising notched and un-notched, specimens were forced-corroded at equal rates using potentiostat. Fig 4.3 shows a typical polarization curve. The pitting potential obtained experimentally is -0.88 V.

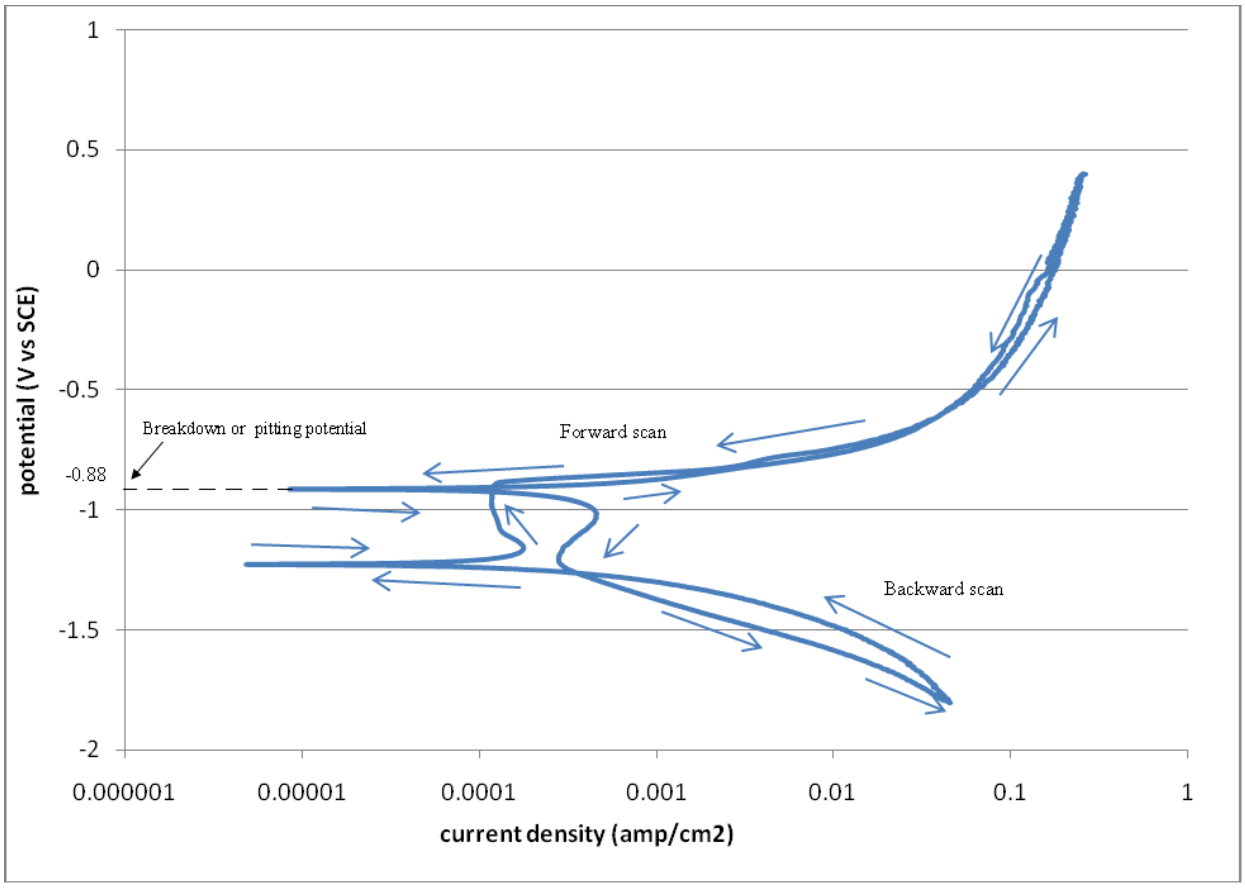

Fig 4.3 Polarization curve from an artificial pit electrode between -1.8 V (SCE) and 0.4 V (SCE) in 3.5% NaCl at a sweep rate of 4.8 mV/s

.

3. The third batch of specimens (un-notched) was forced corroded at different severity rate using potentiostat. Details of forced corrosion scheme are presented as follows:

Table 4.3: Details of forced corrosion at different severities of corrosion

Specimen no.	Voltage range V (SCE)	Current range I (amp/cm^2)	Sweep rate
1	Between -1.8 and 0.4	Between 0.85E-5 and 0.264	4.8 mV/s
2	Between -1.8 and 0.4	Between 1.19E-5 and 0.330	4.8 mV/s
3	Between -1.8 and 0.4	Between 1.80E-5 and 0.247	4.8 mV/s
4	Between -1.8 and 0.4	Between 1.10E-5 and 0.251	4.8 mV/s

A few specimens of each batch were sectioned carefully in the corroded area and examined under optical microscope to visualize the pit size and their distribution. Few rectangular pieces of the alloy were also subjected to corrosion and subsequently examined under optical microscope for pit-density and maximum pit-size measurement.

4.3. Moore Fatigue test:

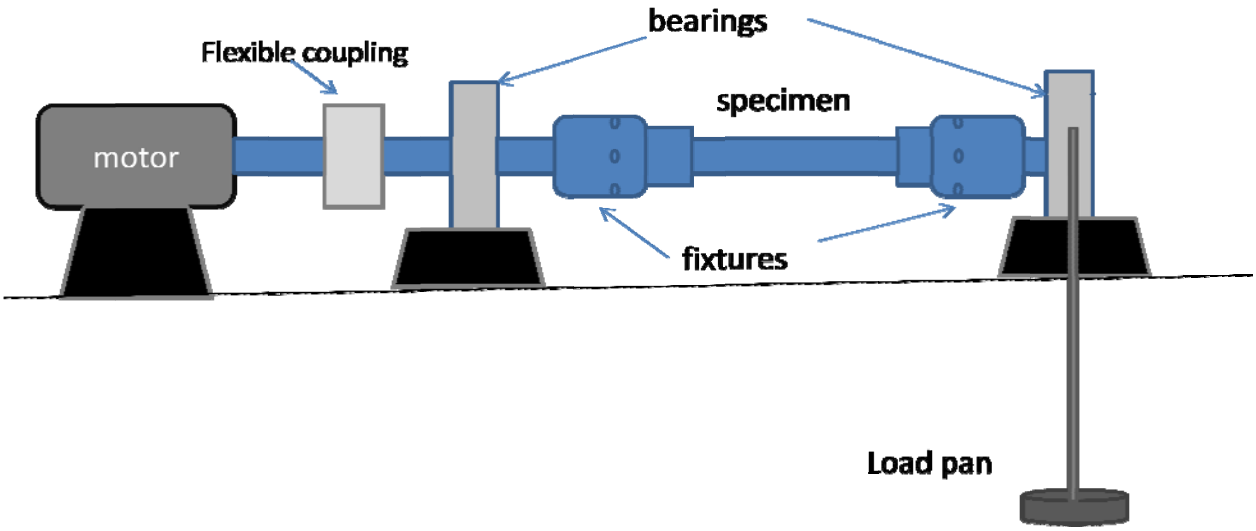

Fig. 4.2 Fatigue testing machine (cantilever type)

A rotating bending machine (RBM) is mostly suitable to test the fatigue properties at zero mean stress. A standard test specimen is clamped in bearings at the ends and loaded at free-end point as shown in Fig 4.2. With this type of device the region of rotating beam between built-in ends is subjected to pure bending with a constant load at its free end. While under the influence of this constant load, the specimen is rotated by the drive spindles around the longitudinal axis; any point on the specimen is thus subjected to completely reversed stress pattern. This test is especially suitable for a condition expected to experience reversible stress pattern. This is also helpful to study crack initiation phenomenon from the surface.

In the present investigation a set of notched specimens were subjected to rotating beam Moore test at a frequency of 100Hz (Stress ratio, R = -1).

The other set of specimens were subjected to uni-axial fatigue test using Instron 8502 servo-hydraulic machine under stress control condition. The tests were conducted at a mean stress, F_{mean}=11.76 kN and a stress ratio(R) =0.2. These tests were conducted in an ambient atmosphere maintaining frequencies of 6Hz. Loading details of both the tests are presented as follows:

Table 4.4: Loading details:

Test type	Loading details			
	Applied Load	Corresponding Maximum stress	Stress ratio (R)	Frequency (f)
Rotating beam fatigue test	4 - 9 kgf (F_{mean}=0)	120.72 - 271.62 MPa	-1	100 Hz
Push- pull test (unnotched specimens)	19.6 kN (F_{mean}=11.76 kN)	250 MPa	0.2	6 Hz
Push- pull test (notched specimens)	12.56 kN (F_{mean}=7.53 kN)	250 MPa	0.2	6 Hz

In order to study the crack initiation phenomenon from the pre-corroded 7020 aluminum alloy specimens the above tests are carried out and fatigue life an *S-N* curves of different specimens are drawn

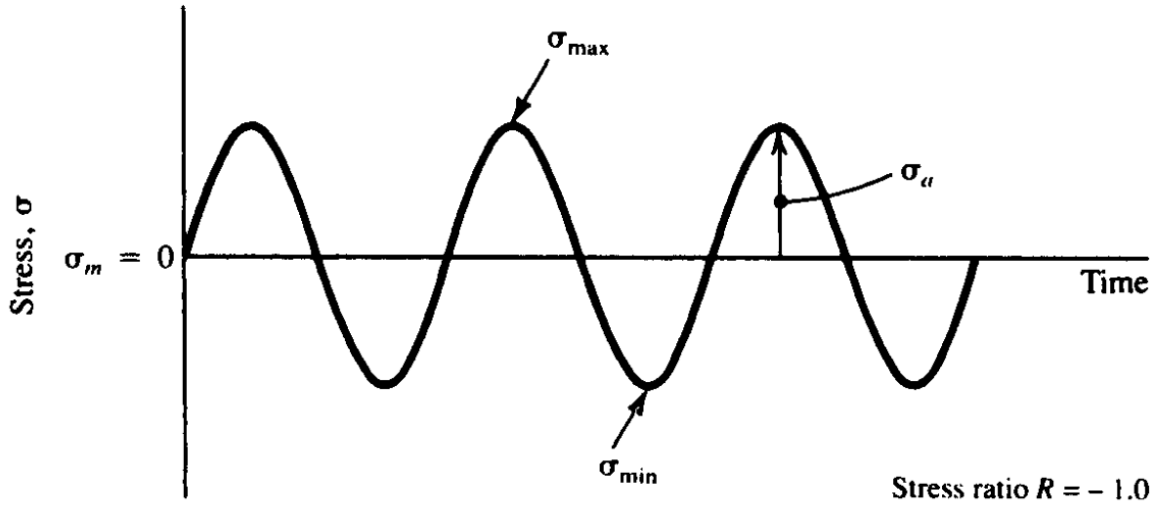

Fig 4.3 Loading cycle in Moore test

4.5. INSTRON-8502 Servo-Hydraulic Dynamic Testing System

Fig 4.4 Instron 8502

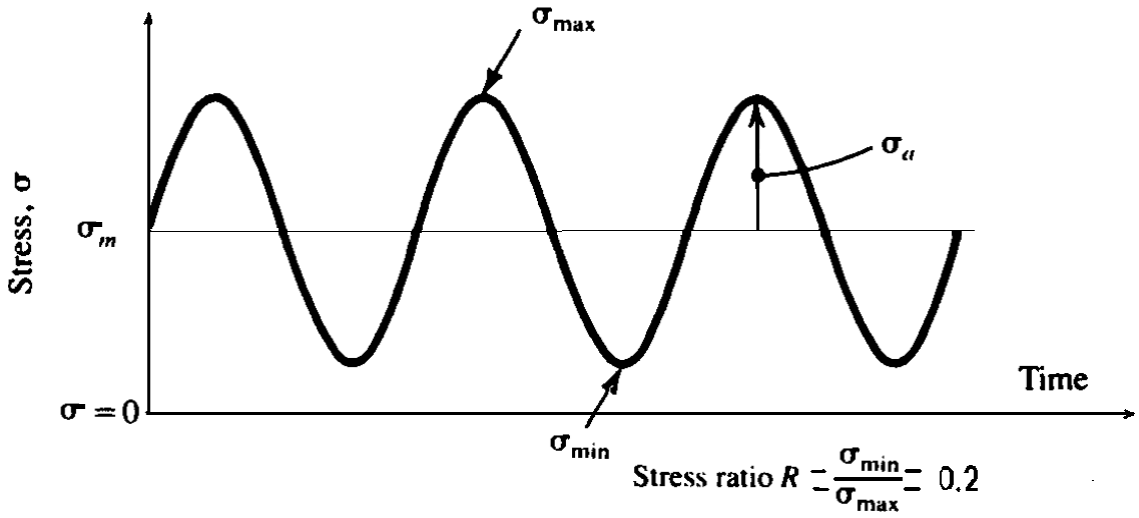

Fig 4.5 Load spectrum for push-pull test

CHAPTER 5

RESULT AND DISCUSSION

Results and Discussion

5.1 Observations for Rotating beam fatigue test

A set of notched specimens were subjected to rotating beam test. The results of the test are tabulated in Table 5.1 and illustrated in Fig. 5.1.

Table 5.1: Rotating beam test data:

S. No	Load (kg)	Bending Stress (MPa)	Notched specimen corrosion condition	No. of cycles to failure (N)
1.	4	120.72	Un-corroded	Did not break upto $1.5x10^7$
			Pre-corroded for 100 hrs	---
			Forced pre-corroded	Did not break upto $3.0x10^7$
2.	5	150.9	Un-corroded	$0.6x10^6$
			Pre-corroded for 100 hrs	$0.9x10^7$
			Forced pre-corroded	$6.6x10^6$
3.	6	181.08	Un-corroded	$1.8x10^7$
			Pre-corroded for 100 hrs	$0.31x10^7$
			Forced pre-corroded	$1.3x10^6$
4.	7	211.26	Un-corroded	$8.9x10^6$
			Pre-corroded for 100 hrs	$0.78x10^6$
			Forced pre-corroded	$5.7x10^6$
5.	8	247.28	Un-corroded	$0.92x10^6$
			Pre-corroded for 100 hrs	$0.6x10^6$
			Forced pre-corroded	---
6.	9	271.62	Un-corroded	$0.88x10^6$
			Pre-corroded for 100 hrs	---
			Forced pre-corroded	---

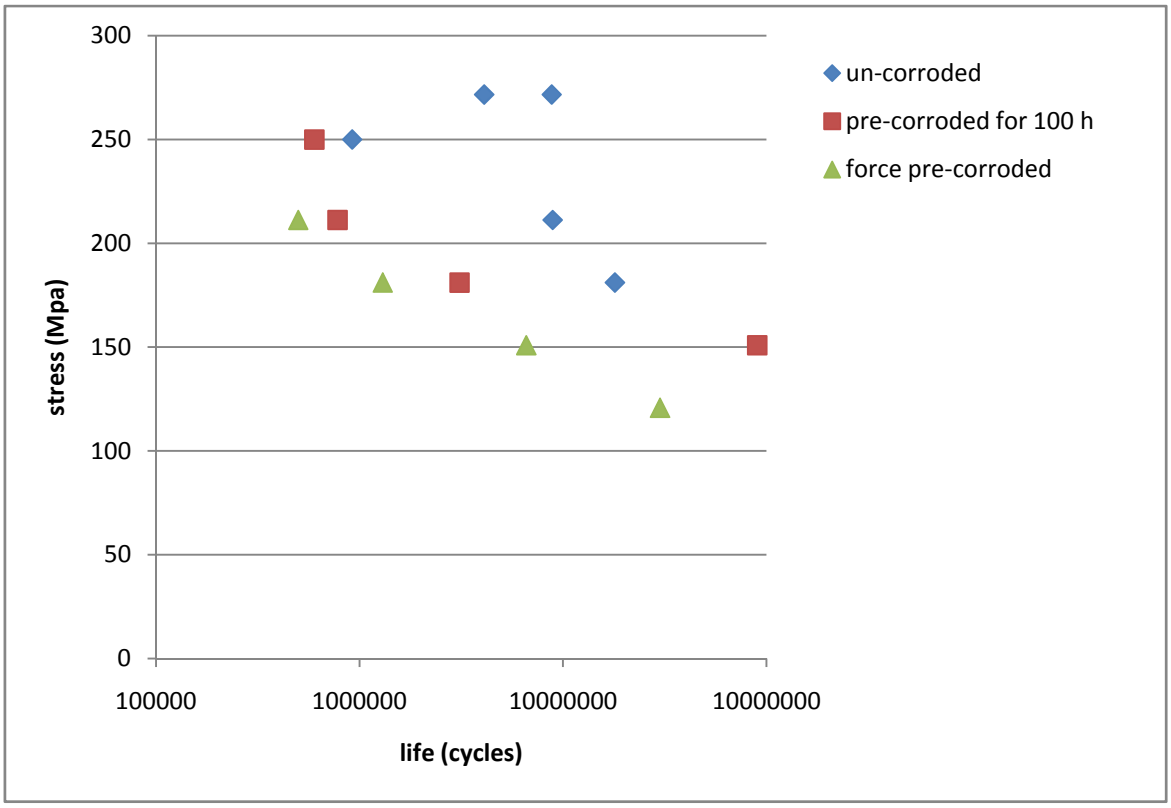

Fig 5.1 *S-N* plot for rotating beam notched specimens

The fatigue life of the alloy is characterized in terms of alternating stress, using experimental data obtained from bending (R = -1) cyclic loading in air and presented in Fig. 5.1. The alloy exhibited a plateau in the stress life plot. It is observed that at an alternating stress level of 250 MPa, the number of cycles to failure is ~8.x10^6, whereas, the life increased to 1.8x10^7on reducing the alternating stress level to 181MPa. A set of notched specimens were subsequently subjected to alternating stress in aqueous solution of NaCl and data are superimposed on air plot. As expected, significant difference between the fatigue behavior in air and saline water is evident. It may be noted that the *S–N* curve has been pulled downwards upon changing the medium from air to saline water. In case of air test, the alternating stress corresponding to a life N_f ~8.9x10^6 is 211 MPa. However, the required alternating stress has been reduced to 160 MPa to maintain the same life in saline water. Significant reduction in the fatigue life in the aqueous solution of NaCl may be partially attributed to the formation of corrosion pits. The corrosion pits on the smooth surfaces of axial loaded specimens may act as stress concentration sites. However, at higher stress level, the crack initiation mechanism may change. The forced corroded specimens are also subjected to rotating beam test and data are also incorporated in the same

figure. In is important to note that the curve has further moved down. This downward shift of the curve is due to increased density of the corrosion pits and their sizes (see Table 5.2).

Table 5.2: Pit densities and maximum size as seen by optical microscope

Corrosion condition	Pit density	Maximum pit size
100 h immersion	24 pits/mm^2	.05 mm mean dia
Forced corrosion	26 pits/mm^2	0.1 mm mean dia

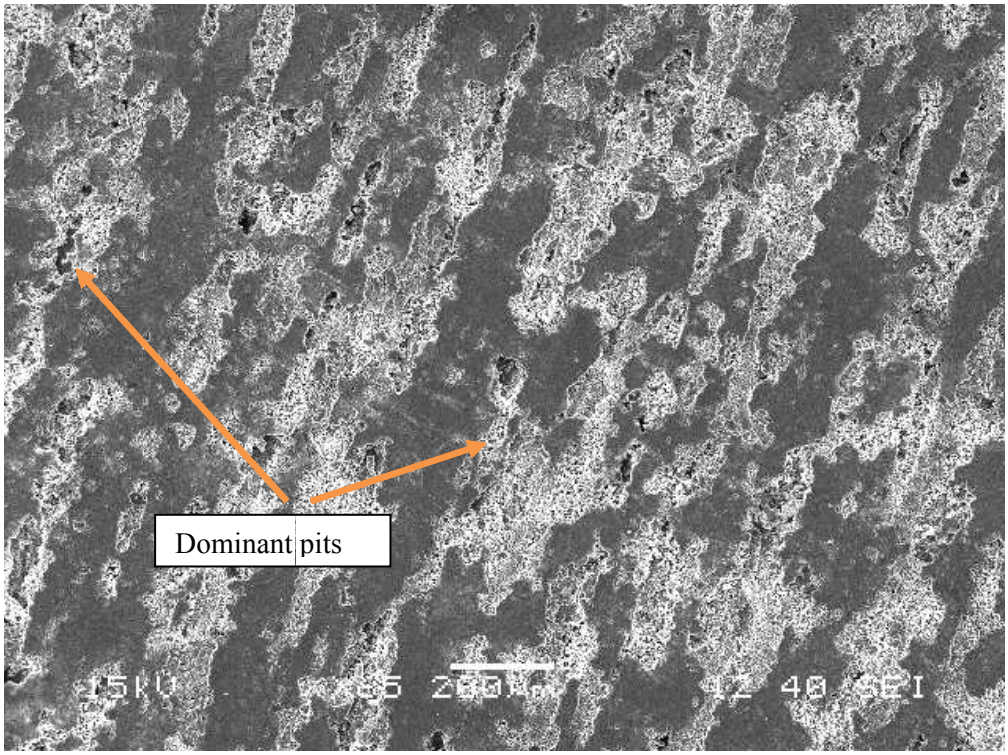

Fig 5.2 SEM showing pit density and size in forced corroded plane surface

The above micrograph (Fig 5.2) shows top view of a forced corroded (-1.8 to 0.4 V, 1.19E-5 to 0.330 mA and 4.8 mV/s scan rate) piece of the alloy. The maximum pit size or size of dominant pit is shown in figure. The specimen is sectioned perpendicular to the surface and scanned for pit depth measurement. The lengths of major and minor axes are shown in the fractrograph (Fig 5.3). The average dimensions of the pits are as shown:

Table 5.3: The average dimensions of pits in forced corrosion specimen

Width (2c)	1.28 mm
Depth (a)	.424 mm

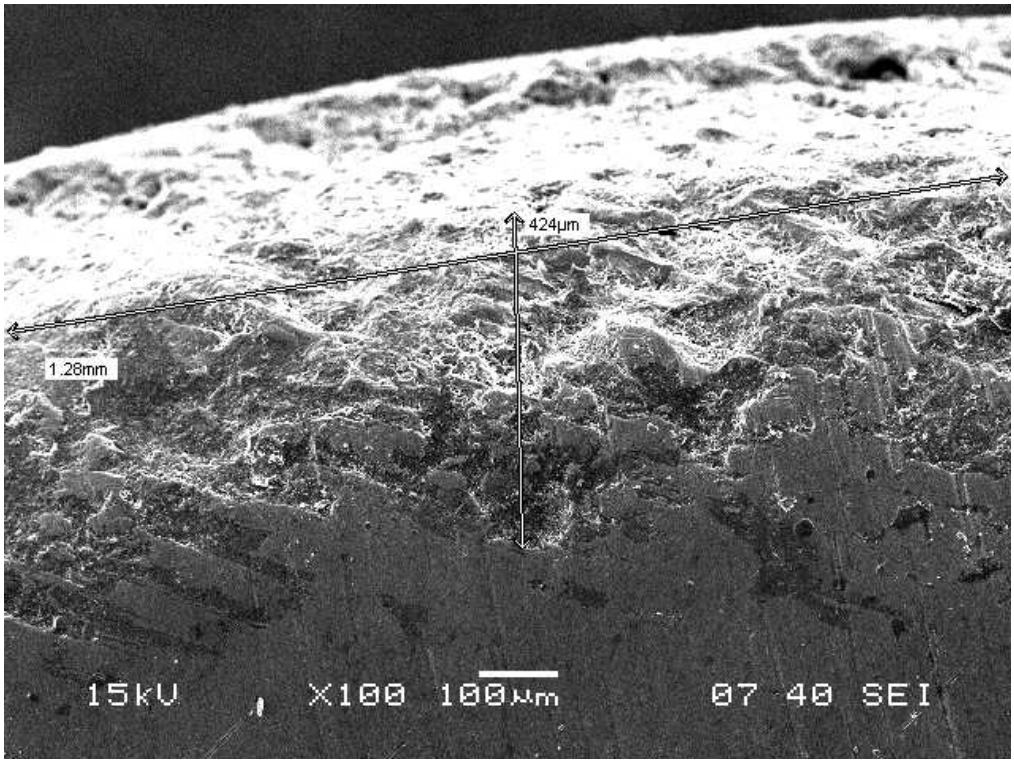

Fig 5.3 SEM visualization of modeling: sectioned forced corroded

5.2 Observations for uni-axial fatigue test:

A set of smooth un-corroded, open circuit corroded and forced corroded specimens were subjected to push-pull test at a fixed stress level (= 250MPa) using INSTRON-8502 testing system. The test results are presented in Table 5.4. Pits formed during the process of corrosion were measured with the help of SEM and SIFs were calculated using eq. (5.1) [5] and presented in the same table. In few cases SIFs were also calculated including the corrosion channel and are also incorporated in the table. The data show reduction in the fatigue with increasing size of corrosion pits. The effect of SIF on fatigue life is also presented in Fig. 5.4

Relation used to calculate SIF:

$$K_I = \frac{1.12\sigma\sqrt{\pi b}}{\frac{3\pi}{8} + \frac{\pi}{8}\left(\frac{b}{c}\right)^2} \qquad (5.1)$$

Where, K_I= stress intensity factor for push pull test (I indicates mode I)

σ= maximum stress=250 MPa.

b=depth of pit (minor axis of elliptical model)

c=pit opening dia (major axis of elliptical model)

Table 5.4: Push-pull test data

S. No	Particulars of specimen	Stress intensity factor(SIF) based on fractrograph (MPa/.m$^{1/2}$)		Cycles to fail
		Without corrosion channel	With corrosion channel	
1	Forced pre-corrosion, Un-notched	11.347	10.243	25469
2	Forced pre-corrosion, Un-notched	13.47	13.287	22853
3	Forced pre-corrosion, Un-notched	13.325	13.705	22722
4	Forced pre-corrosion, Un-notched	14.163	-----	19008
5	Forced pre-corrosion, Notched	7.56	-----	17521
6	100 h pre-corrosion, Notched	0.999	-----	25884
7	Un-corroded, Un-notched	-----	-----	94541
8	Un-corroded, Notched	-----	-----	10186

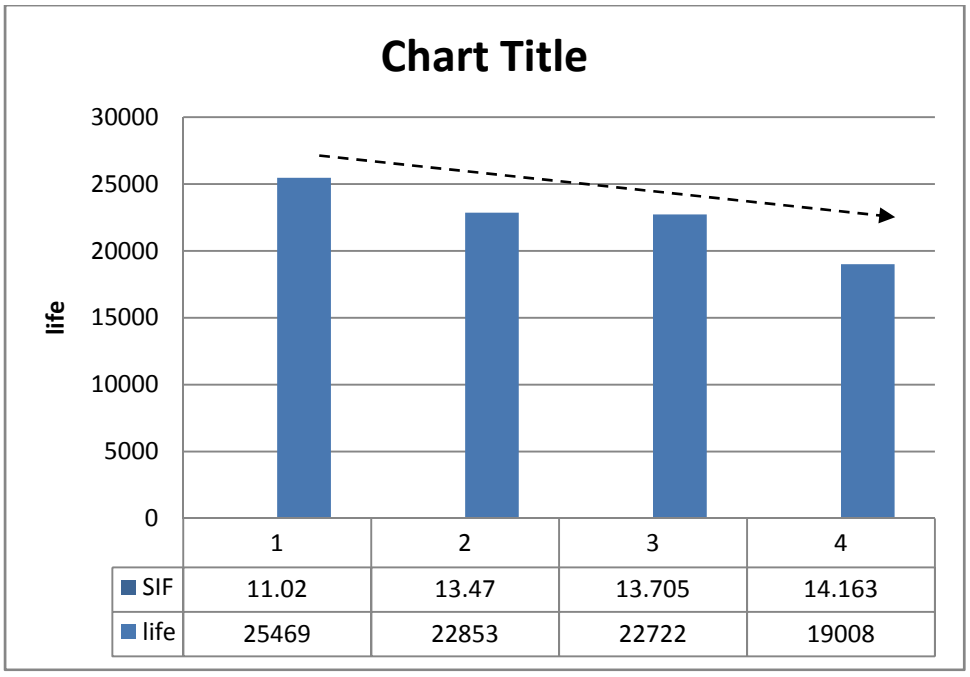

Fig 5.4 Bar chart for uni-axial fatigue tests for smooth samples

5.3 Fractographs:

5.3.1 100 h corroded notched sample

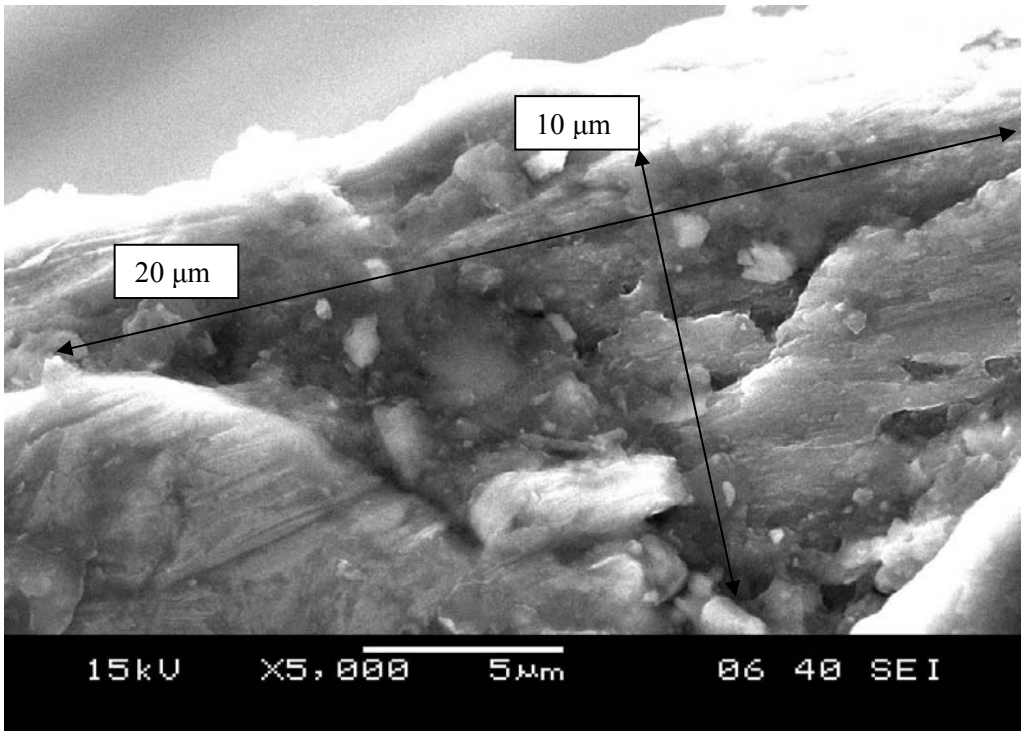

Fig 5.5 Fractograph of specimen subjected to pre-corrosion (open circuit corrosion for100 hrs). Fatigue crack initiation from corrosion pit can be visualized.

The fractured surface of 100 h pre-corroded sample was examined under SEM and presented in Fig 5.5. The corrosion products and pit size are clearly visible and the pit size. The careful examination of the fracture surface indicated crack initiation from the pit. The measured dimensions of the above pit are presented in Table 5.5. A small area close to this pit was X-ray examined and EDS plot is presented in Fig. 5.6. High amount of chlorine along with Fe, Si and Mn indicate a galvanic cell formation and accelerated corrosion at a site containing impurities.

Table 5.5: pit dimensions in 100 h notched corroded specimen

Width (2c)	0.02 mm
Depth (a)	0.01 mm

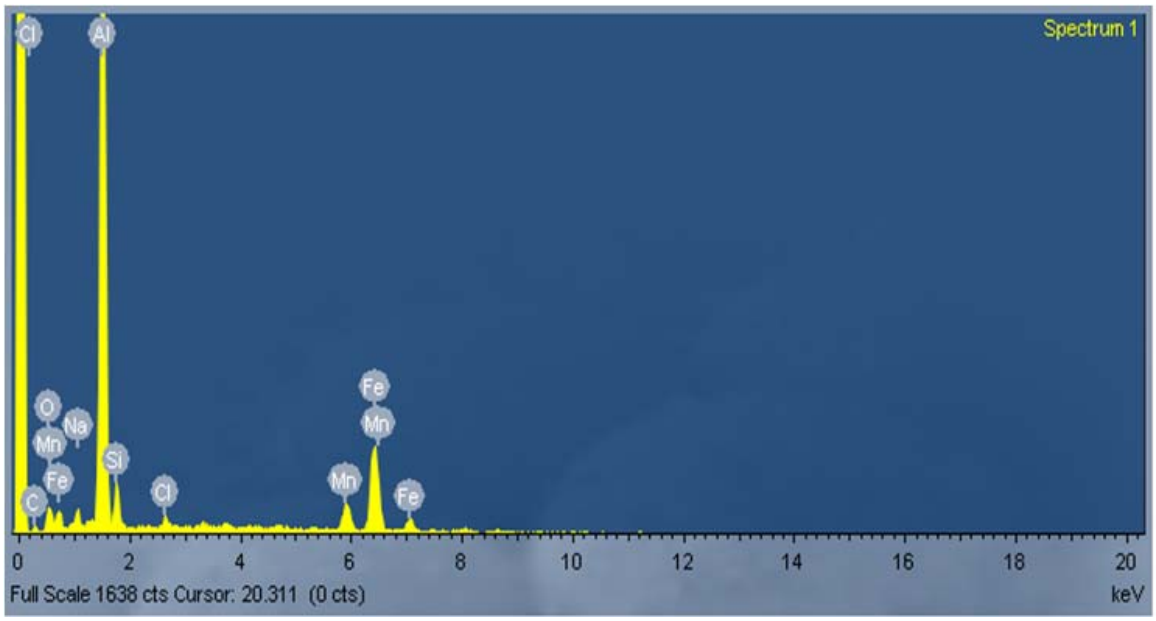

Fig 5.6 EDS plot showing corrosion in initiation point

Fractograph of smooth and forced corroded specimen are presented in Figs. 5.7 to 5.14. Fig. 5.7 shows an elliptical damaged zone formation near the surface of the specimen. The magnified view of a region close to the surface shows the corrosion product formation. On the basis of Fig 5.5 it may be noted that there is also sign of galvanic corrosion. The mud structure also reviles the presence of corrosion products. Figs. 5.9 and 5.11 show the corrosion channel deep into the specimen. A spot of this channel was also revealed the oxidation of the material during its exposure to the environment. Fig.5.10 shows the magnified view of a zone close to the corrosion channel. The fatigue striations do not appear ductile in nature. This may be due to the presence of chemical spices and high strain (stress concentration induced) due to the close proximity of the channel. Fractograph at a distance 1.4mm from the surface and 0.05mm from a channel overload induced microvoids and ductile striations (Fig. 5.12). These microvoids are indication of high strain development near the channel. However, the fractograph at a distance 2.77mm from the surface shows ductile striations dominated crack extension (Fig. 5.13). Fig.5.14 shows overload fracture at a distance of 3.45 mm from the surface. Relatively large pits can be seen in the fractrograph of un-notched forced corroded specimens. Usually these pits are followed by long corrosion channels (Fig 5.8) with muddy appearance which confirms the inter-granular corrosion has resulted those channels. These corrosion channels can also be approximately modeled into elliptical pits as shown in Fig 5.7. The dimensions of the pits are as shown:

Table 5.6: pit dimensions in un- notched forced corroded specimen 1

	Without corrosion channel	With corrosion channel
Width(2c)	1.59 mm	2.58 mm
Depth (a)	.962 mm	1.3 mm

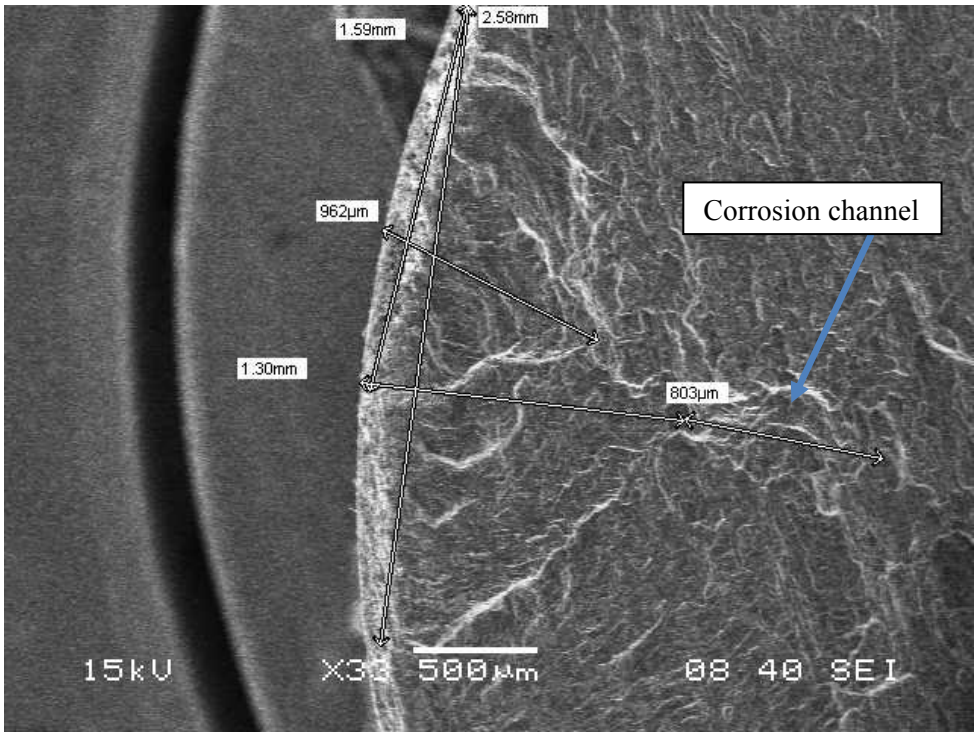

Fig 5.7 Pit dimensions in forced corroded sample 1

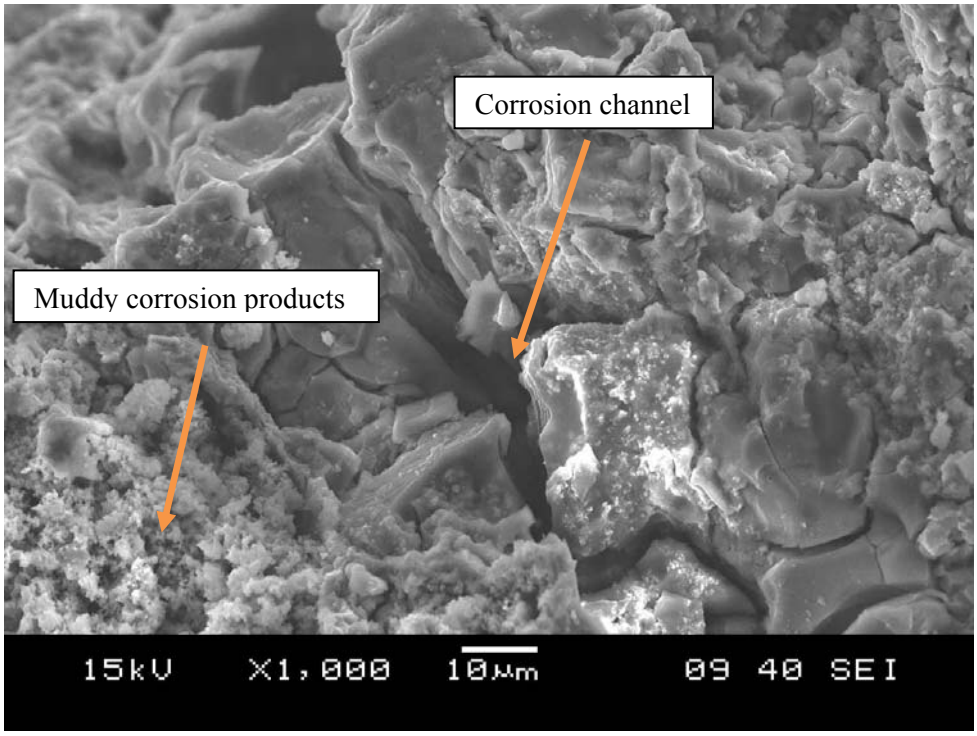

Fig 5.8 SEM showing corrosion products at pit in forced corrosion

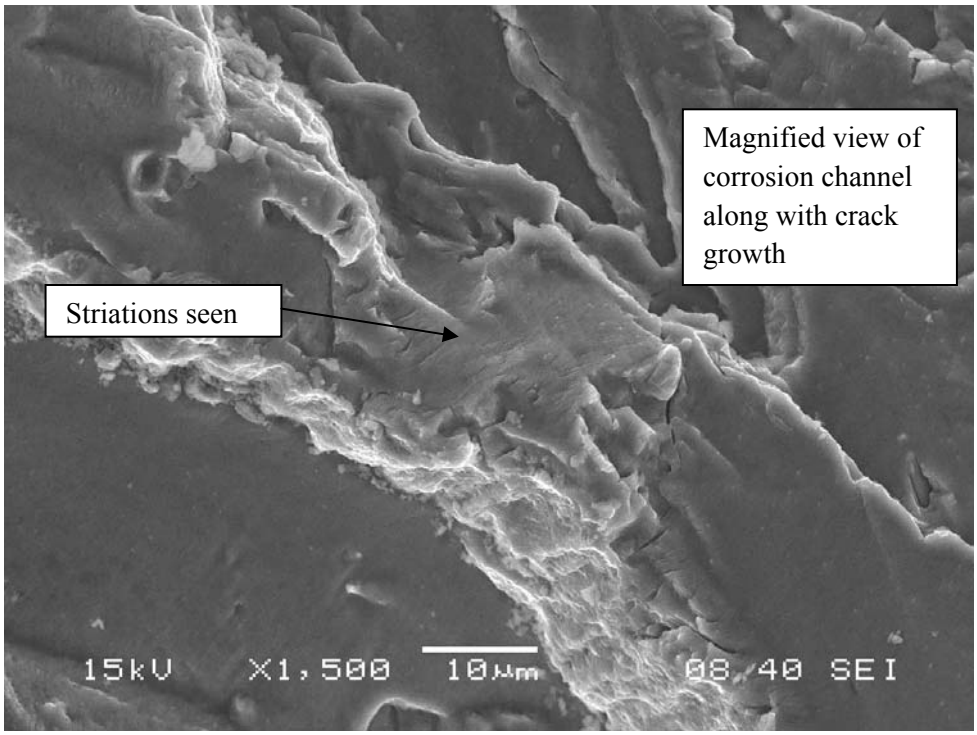

Fig 5.9 Corrosion channel seen in SEM along crack length

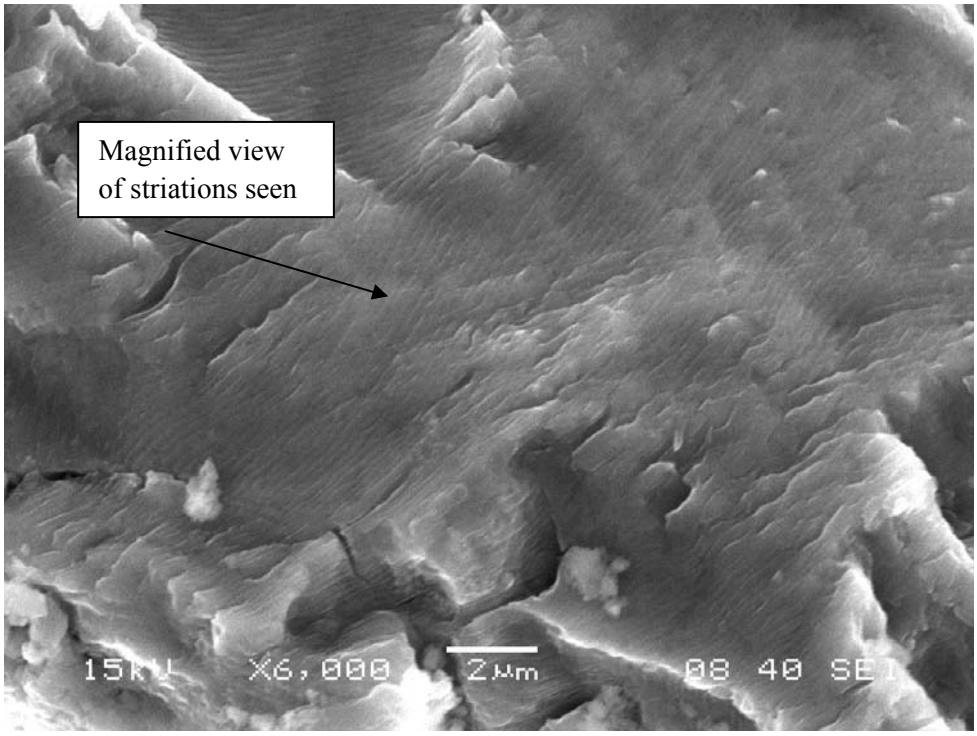

Fig 5.10 SEM showing striations at a distance 803µm

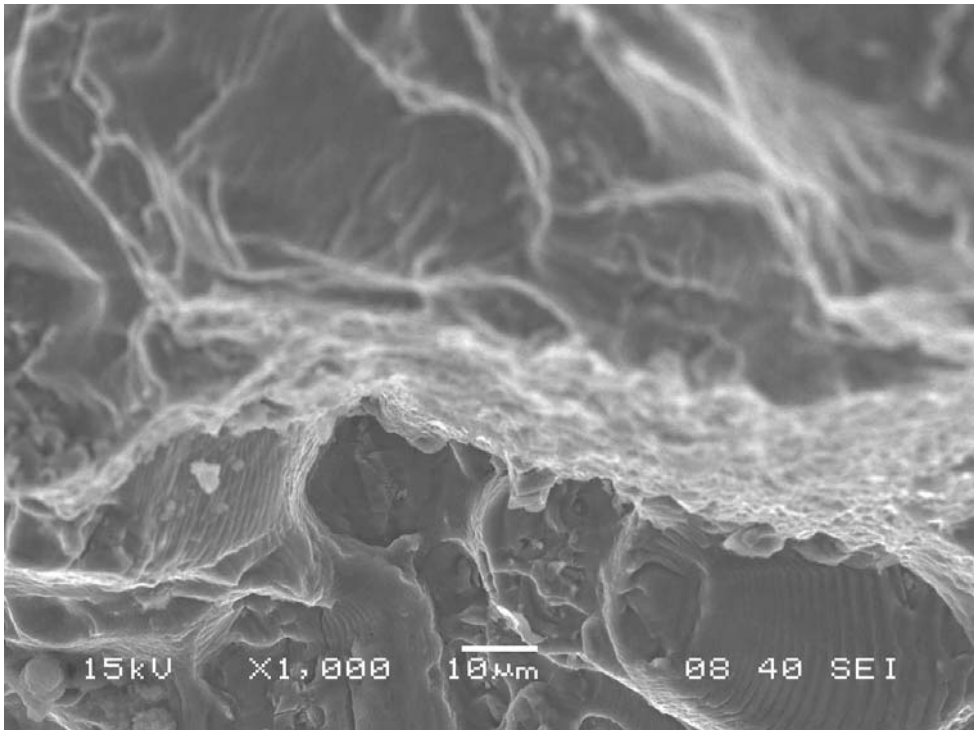

Fig 5.11 Corrosion channel affecting crack growth

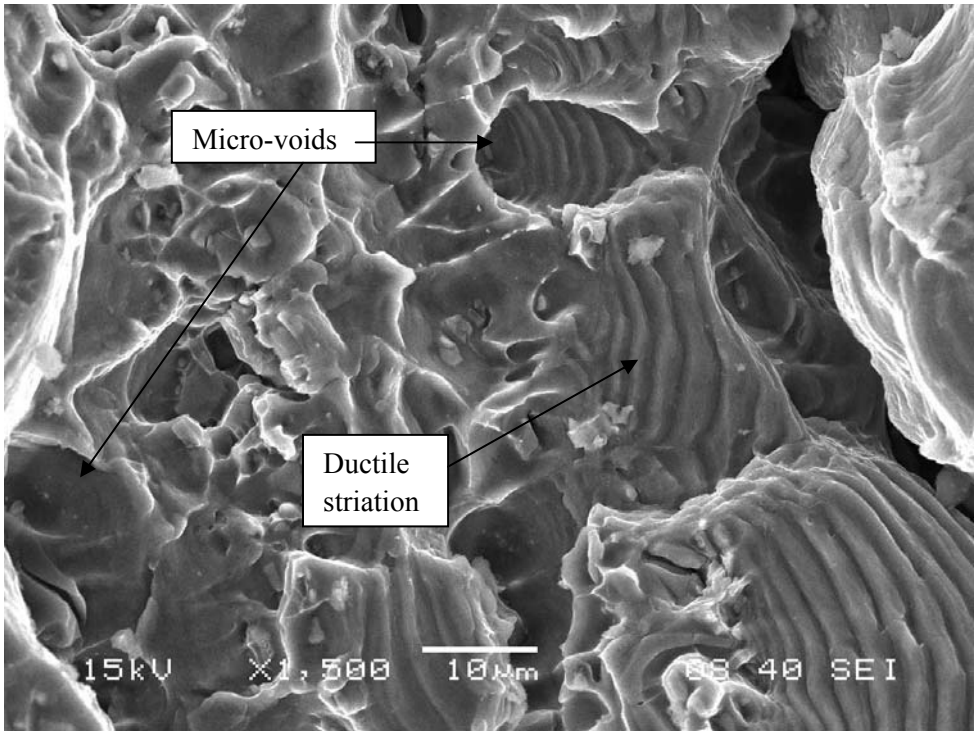

Fig 5.12 micro-voids seen along crack length (less in number) at 1.40 mm from surface

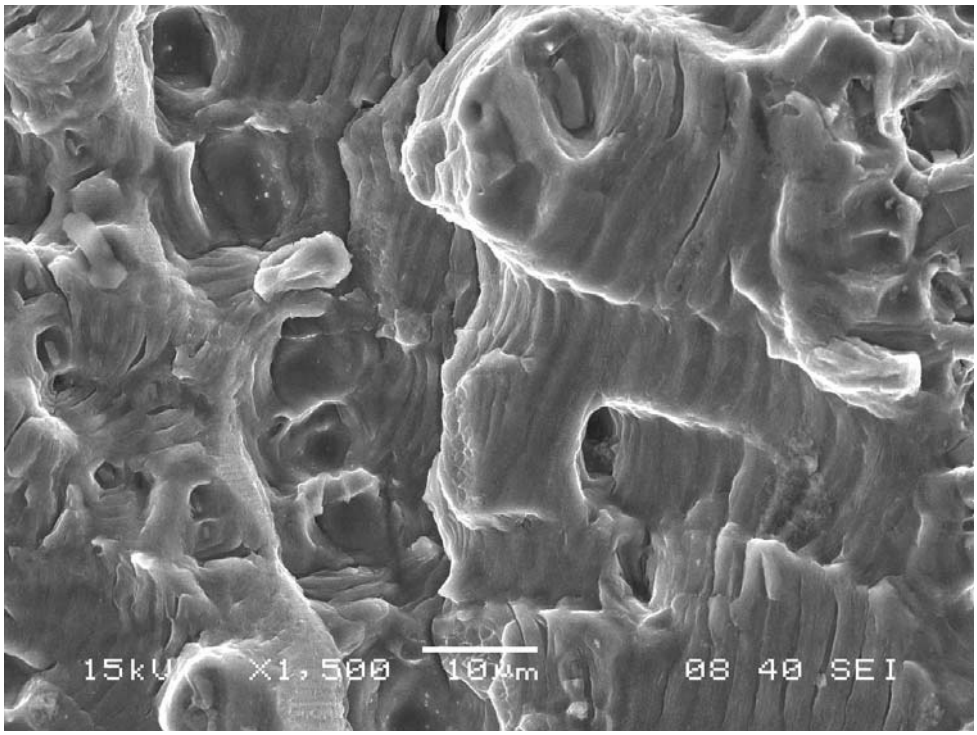

Fig 5.13 micro-voids increases in number shows ductile tearing at 2.77 mm from surface

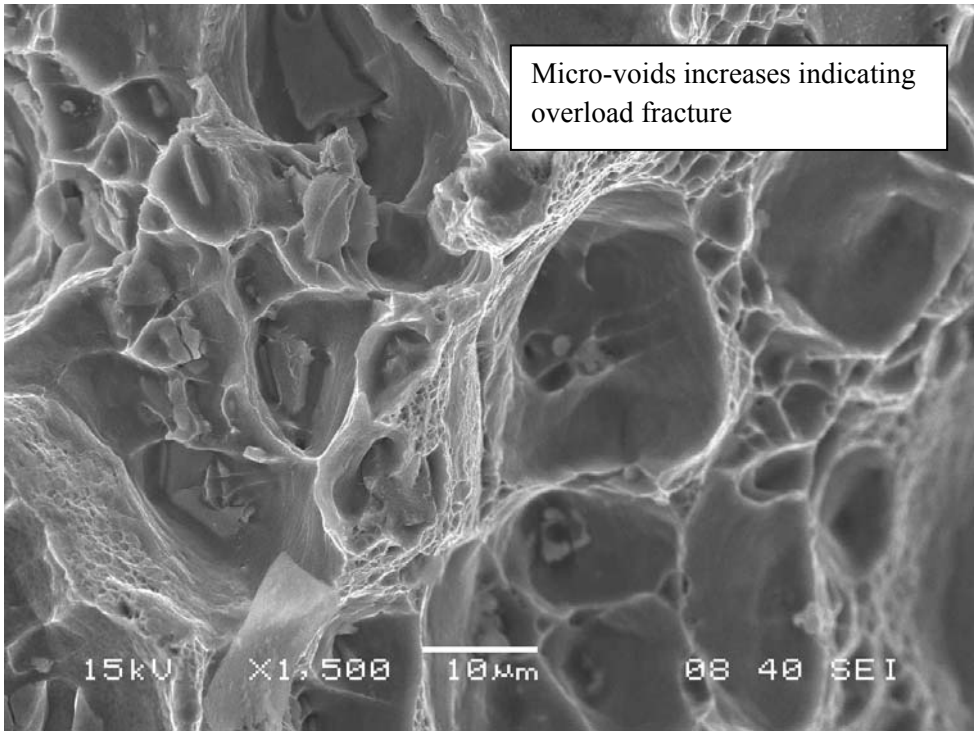

Fig 5.14 Dimpled structure showing overload fracture at 3.45 mm from surface

5.3.2 Notched un-corroded: In un-corroded specimens, crack initiation point cannot be distinctly seen; the main feature seen was cyclic cleavage, as shown in figure

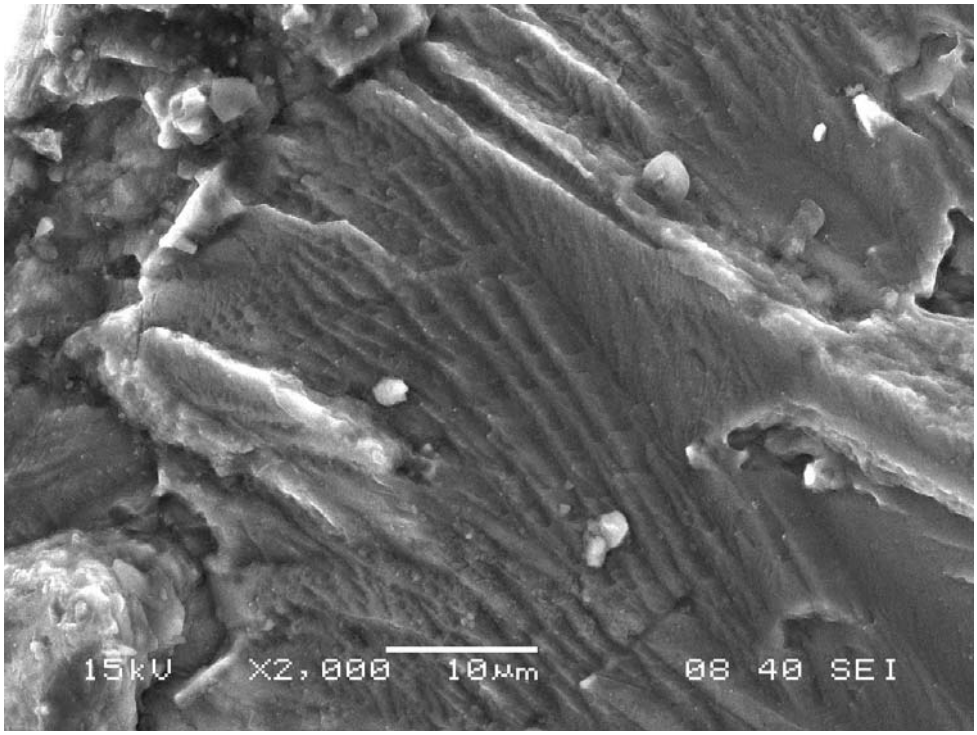

Fig 5.15 Cyclic cleavage containing striation

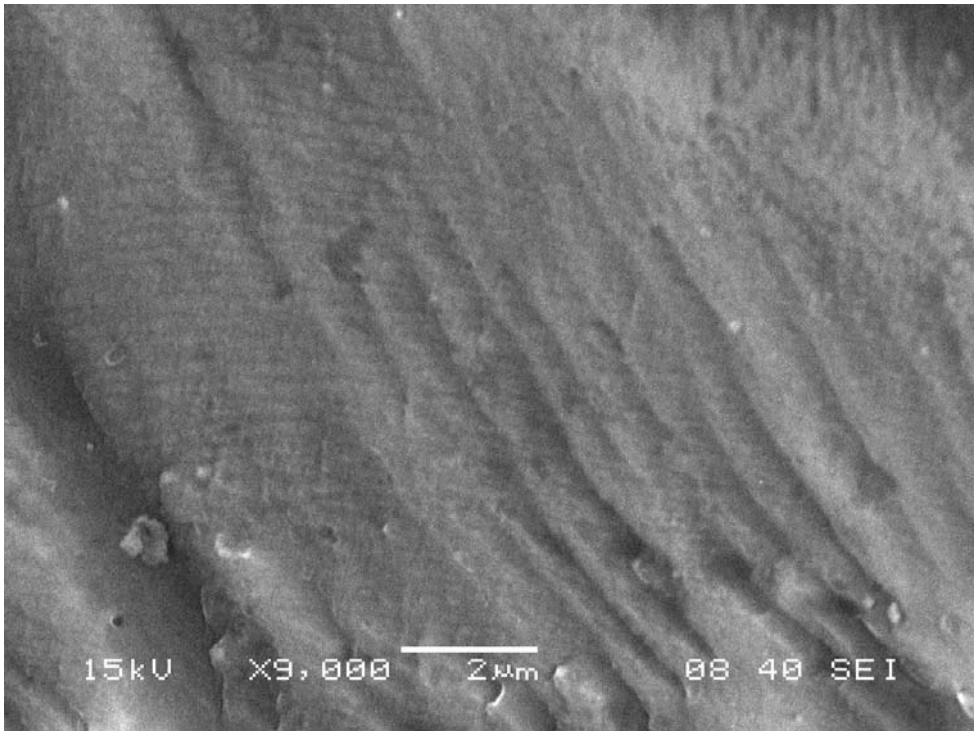

Fig 5.16 Cyclic cleavage containing striation at higher magnification

5.3.3 Un-notched forced corroded sample 2:

Table 5.7: pit dimensions in un- notched forced corroded specimen 2

	Without corrosion channel	With corrosion channel
Width(2c)	3.65 mm	3.65 mm
Depth (a)	1.69 mm	2.23 mm

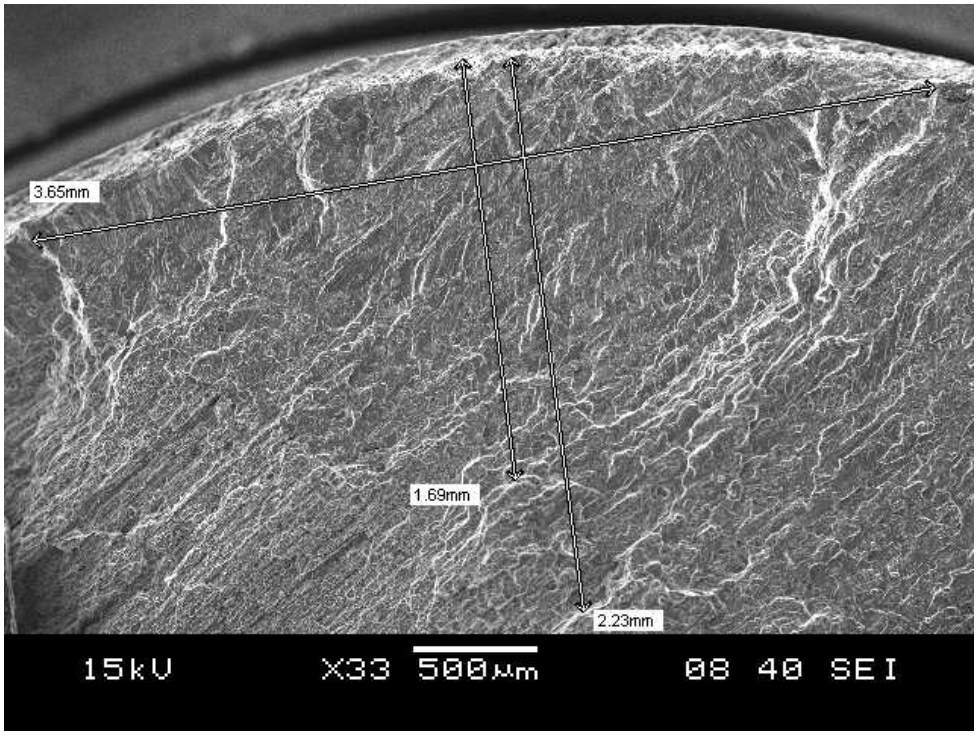

Fig 5.17 Pit dimensions un-notched forced corroded sample 2

5.3.4 Un-notched forced corroded sample 3:

Table 5.8: pit dimensions in un- notched forced corroded specimen 3

	Without corrosion channel	With corrosion channel
Width (2c)	3.78 mm	3.78 mm
Depth (a)	1.40 mm	1.75 mm

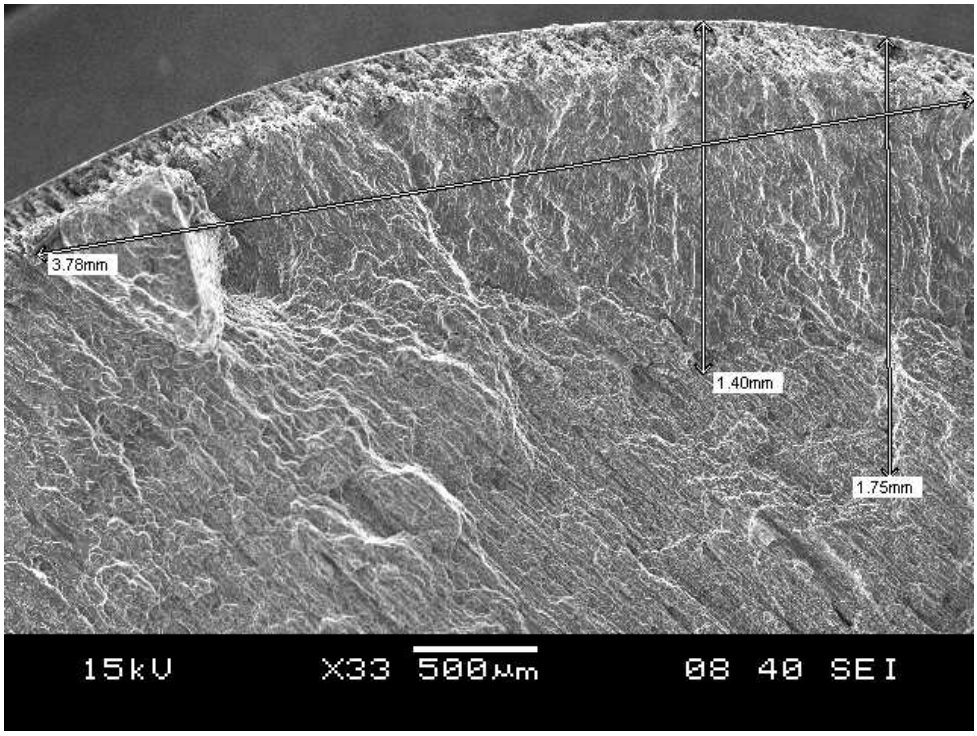

Fig 5.18 Pit dimensions un-notched forced corroded sample 3

5.3.5 Un-notched forced corroded sample 4:

Table 5.9: pit dimensions in un- notched forced corroded specimen 4

	Without corrosion channel	With corrosion channel
Width(2c)	4.5 mm	---
Depth(a)	1.48 mm	---

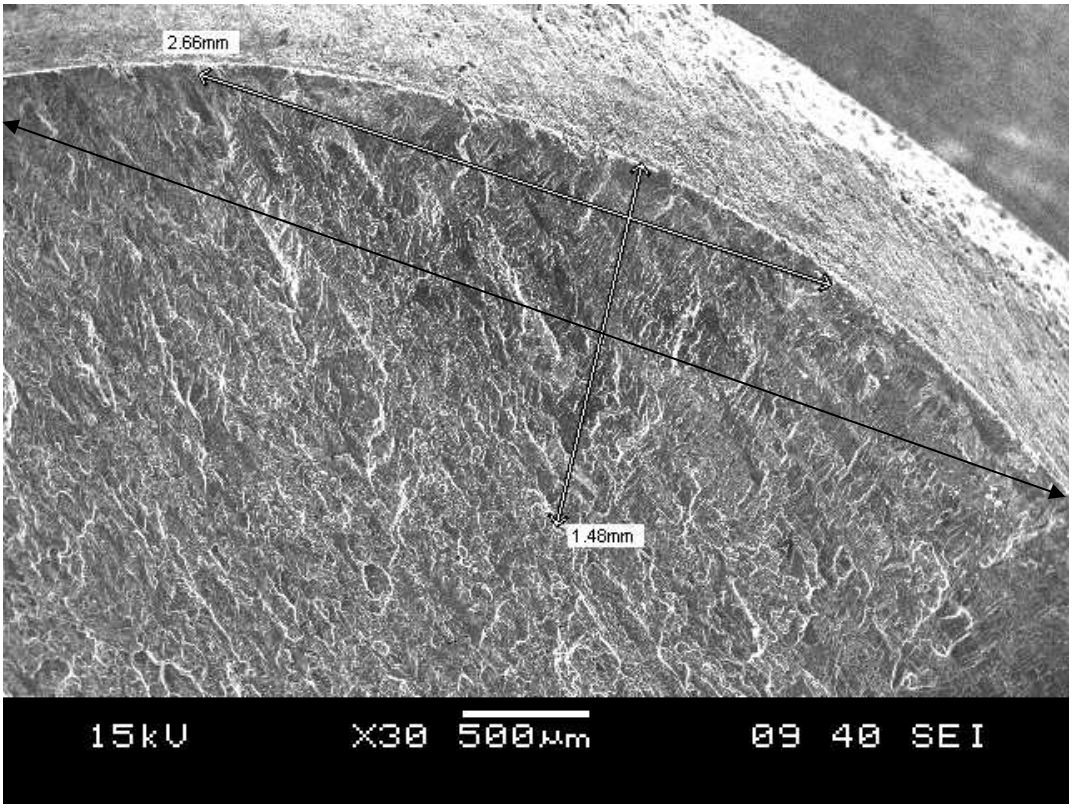

Fig 5.19 Pit dimensions un-notched forced corroded sample 4

Figs. 5.20 -5.22 show the fractographs of smooth un-corroded specimen It can be clearly seen that the fatigue failure occurred as a consequence of cracks nucleated at the periphery of the specimen and did not initiate from any surface inclusion. It is observed that the flat and featureless facets, located on the specimen surface appear to be the origin of stage-I crack. The featureless crack extension is followed by cyclic cleavage, a slow crack growth region [12, 19]. The above features of the fracture surface are indication of low crack growth extension and high-energy fracture at low ΔK level. The ductile striations induced crack extension can be visualized in Fig. 5.22.

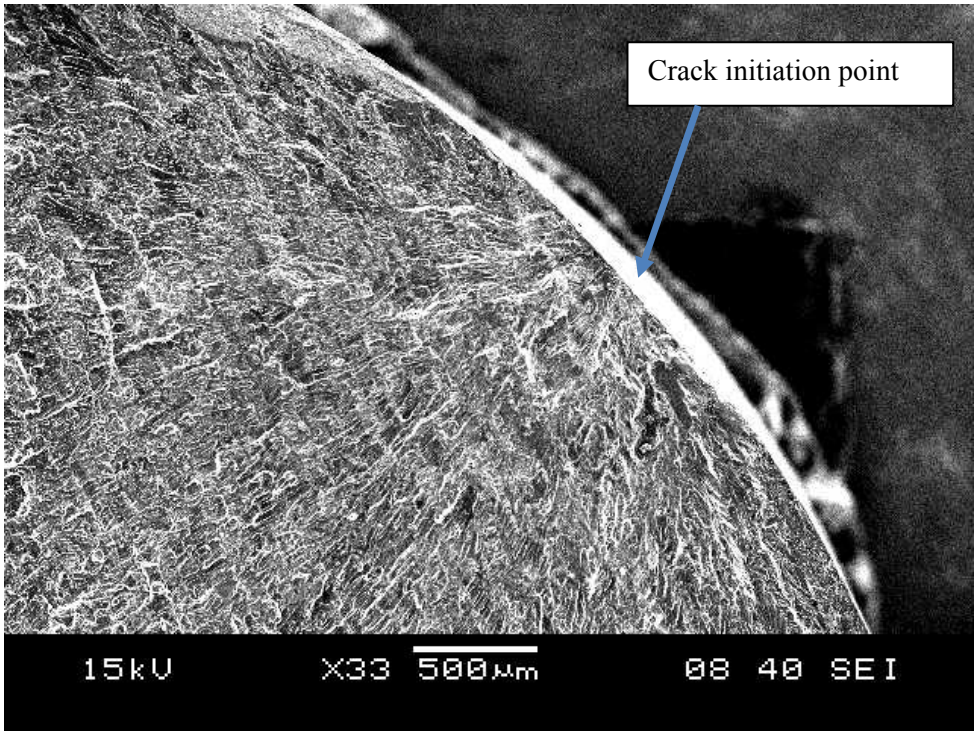

Fig 5.20 Crack initiation point of un-corroded un-notched specimen

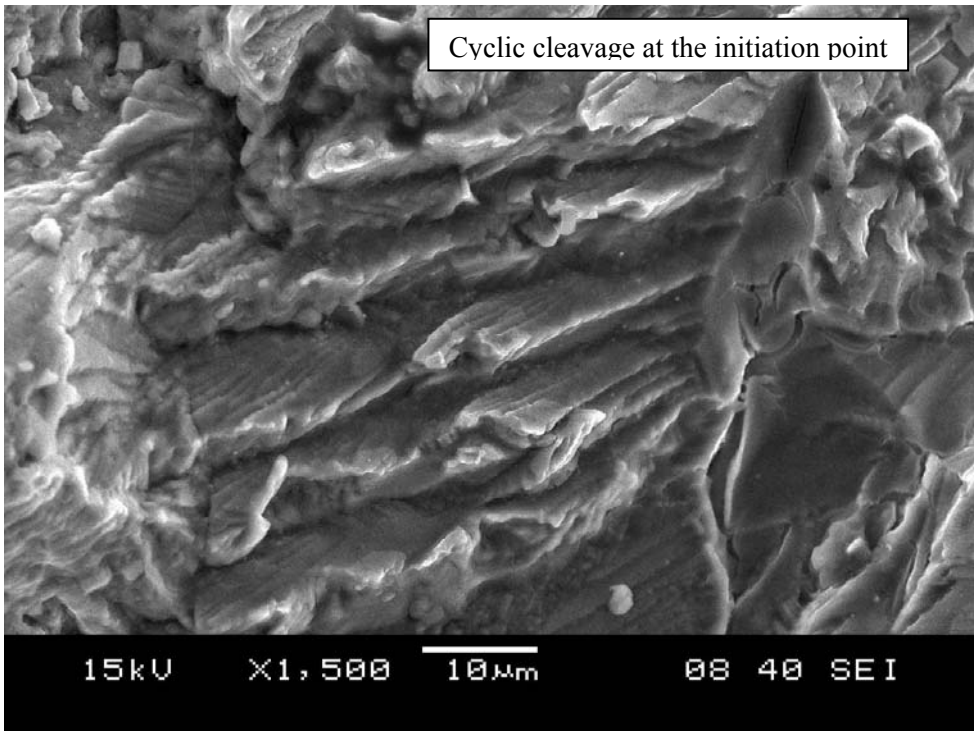

Fig 5.21 Cyclic cleavage at higher magnification

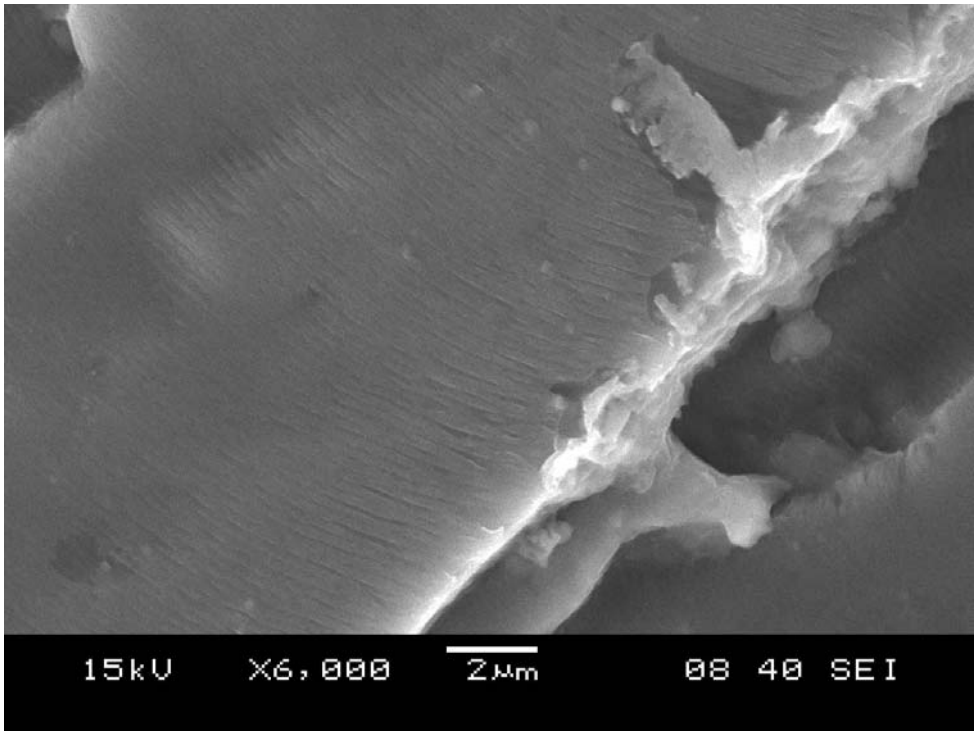

Fig 5.22 Brittle striations seen at further higher magnifications

CHAPTER 6

CONCLUSIONS AND FUTURE WORKS

6.1 Conclusion

1. The fatigue life of 7020-T7 aluminum alloy is reduced significantly by pre-corrosion in an aqueous solution of sodium chloride.
2. Corrosive environmental exposure of the alloy initiated corrosion pits on the surface. The fracrographic observation indicated initiation of crack from corrosion pits in case of pre-corroded specimens. However, the flat and featureless facets, located on the specimen surface appear to be the origin of stage-I crack in un-corroded specimens. The featureless crack extension is followed by cyclic cleavage, a slow crack growth region.
3. Deep fatigue channels are also observed in the pre-corroded specimens. These channels may have accelerated the crack growth and altered the mode of fracture.
4. The stress intensity factors, calculated based on equivalent elliptical corrosion pits, show good agreement with the fatigue life in case of smooth specimens.

6.2 Future work

1. Large number of specimens may be tested to develop *S-N* curve.

2. The corrosive environment is also known to affect crack growth rate. Therefore, an attempt may be made study the effect of environment on crack growth of pre-corroded specimen.

3. A corrosive environment is also known to affect crack growth behavior. Therefore, alloy may be subjected to a true environmental fatigue test within a suitable arrangement e.g. a corrosive environment in a close chamber.

References:

[1] Verma B.B., Atkinson J D and Kumar M, Study of fatigue behavior of 7475 aluminum alloy, Bulletin of Materials Science, Volume 24, (2001):231-236

[2] Jacob M.S.D, Arora Prithvi Raj, Saleem M., Mahdi Ahmed Elsadig, Sapuan S.M. Fretting fatigue crack initiation: An experimental and theoretical study, International journal of fatigue , Volume 29,(2007):1328-1338

[3] Jean Mark P.Genkin, PhD thesis, Corrosion fatigue performance of alloy 6013-T6, Massachusetts Institute of Technology, (1994)

[4] Wilson de Jesus, Marinalda Claudete Pereira, Roberto Zenhei Localised corrosion of 7XXX aluminum alloys in chloride media, Technical Contribution to the xxst International Congress of the ABM, Rio de Janeiro – RJ – Brazil, (January 2007)

[5] Suresh S., Fatigue of materials, Cambridge university press, II Edition.

[6] Berkeley D. W., Sallam H. E. M. and H. Nayeb-Hashmi, The effect of pH on the mechanism of corrosion and stress corrosion and degradation of mechanical properties of AA6061 and NEXTEL 440 fiber-reinforced AA6061 composite, Corrosion Science Volume 40, Issues 2-3, (February-March 1998):141-153

[7] Cheng W, Cheng HS, Mura T, Keer LM. Micromechanics modeling of crack initiation under contact fatigue. ASME J Tribol, 116, (1994):2–8.

[8] An Introduction of mechanical Testing, http://materials.open.ac.uk/mem/mem_mftext.htm

[9] Mura, Nakasone, A theory of fatigue crack initiation in solids. J Appl Mech, 57, (1990):1–6.

[10] Li X.-M. and Starink M. J., The Effect of Compositional Variations on the Characteristics of Coarse Intermetallic Particles in Overaged 7xxx Al Alloys, Mater. Sci. Techn, Volume 17, (2001): 1324-28

[11] Silverman David C., Tutorial on polexpert and the cyclic potentiodynamic polarization technique. http://www.argentumsolutions.com/tutorials/polexpert_tutorialpg3.html.

[12] V. Lamacq, M.C. Dubourg and L. Vincent, A theoretical model for the prediction of initiation growth angles and sites of fretting fatigue cracks, Tribol Int 30 (1997):391–400

[13] Pyun Su-Il, Orr Seung-Jin, Nam Soo-Woo, Corrosion fatigue crack initiation of Al–Zn–Mg–Mn alloy in 0.5 M Na2SO4 solution, Materials Science and Engineering A241, (1998):281–284

[14] Medved J.J, Breton M., Irving P.E, Corrosion pit size distributions and fatigue lives—a study of the EIFS technique for fatigue design in the presence of corrosion. International Journal of Fatigue, 26, (2004):71–80

[15] Genel K., The effect of pitting on the bending fatigue performance of high-strength aluminum alloy Scripta Materialia 57, (2007):297–300

[16] Sander M., Richard H.A., Lifetime predictions for real loading situations—concepts and experimental results of fatigue crack growth, International Journal of Fatigue, 25, (2003):999–1005

[17] Pao P.S., Gill S.J. and Feng C.R, On fatigue crack initiation from corrosion pits in 7075-T7351 aluminum alloy Scripta mater. 43, (2000):391–396

[18] Szklarska-Smialowska Z, Pitting corrosion of aluminum, Corrosion Science 41, (1999): 1743-1767

[19] García-Romero A, Delgado A., Urresti A., Martín K., Sala J.M., Corrosion Behavior of Several Aluminum Alloys in Contact with a Thermal Storage Phase Change Material Based in Glauber´s Salt, Corrosion Science, (2008): 1263-1272

[20] Ning Liu, Jianli Wang, Lidong Wang, Yaoming Wu, Limin Wang, Electrochemical Corrosion Behavior of Mg-5Al-0.4Mn-xNd in NaCl Solution, Corrosion Science,(2008): 1328-1333

[21] Munoz A.G, Saidman S.B., Bessone J.B., Corrosion of an Al–Zn–In alloy in chloride media, Corrosion Science 44, (2002):2171–2182

[22] S Shuangqing, Zheng Qifei, Li Defu, Wen Junguo, Long-term atmospheric corrosion behavior of aluminum alloys 2024 and 7075 in urban, coastal and industrial environments, Corrosion Science 51, (2009):719–727

[23] Chen G.S., Wan K.-C., Gao M., Wei R.P. and Flournoy T.H., Transition from pitting to fatigue crack growth—modeling of corrosion fatigue crack nucleation in a 2024-T3 aluminum alloy, Materials Science and Engineering , Volume 219, Issues 1-2(1996):126-132

[24] Najjar D., Magninand T., Warne T. J., Influence of critical surface defects and localized competition between anodic dissolution and hydrogen effects during stress corrosion cracking of a 7050 aluminum alloy, Materials Science and Engineering, Volume 238, Issue 2 , (1997):293-302

[25] Harlow D. G. and Wei R. P., A probability model for the growth of corrosion pits in aluminum alloys induced by constituent particles, Engineering Fracture Mechanics Volume 59, Issue 3, (1998):305-325

[26] Rudd, J.L. and T.D. Gray, Quantification of Fastener-Hole Quality, Journal of Aircraft,. 15(3), (1978):143-147.

[27] Shekhter A., Loader C., Hu W. and Crawford B. R. ,Assessment of the Effect of Pitting Corrosion on the Safe Life Prediction of the P-3C. Air Vehicles Division DSTO Defense Science and Technology Organization 506 Lorimer St Fishermans Bend, Victoria 3207 Australia, (2007)

[28] Yang C. Y., Liaw, P. K. Palusamy S. S., and Ren W.,S-N Curve for Crack Initiation and an Estimate of Fatigue Crack Nucleus Size, Fatigue and Fracture Mechanics, Volume 27(1997):352-364

[29] Shih Y.S. and Chen J.J., The stress intensity factor study of an elliptical cracked shaft, Nucl Eng Des 214 (2002):137–145.

[30] Couroneau N. and Royer J., Simplified model for the fatigue growth analysis of surface cracks in round bars under mode I, Int J Fatigue 20 (1998):711–718.

[31] Shi Pan and Mahadevan Sankaran, Damage tolerance approach for probabilistic pitting corrosion fatigue life prediction, Engineering Fracture Mechanics, Volume 68, Issue 13(2001):1493-1507

[32] Chubb J.P., Morad T.A, Hockenhull B.S. and Bristow J.W., The effect of exfoliation corrosion on the fracture and fatigue behavior of 7178-T6 Aluminum , International journal of Fatigue, Volume 17, No. 1,(1995):49-54

[33] Kimberli Jones, Shinde Sachin R., Clark Paul N., Hoeppner David W., Effect of prior corrosion on short crack behavior in 2024-T3 aluminum alloy, Corrosion Science 50, (2008):2588–2595

[34] Langer, B. F., "Design of Pressure Vessels for Low-Cycle Fatigue," Journal of Basic Engineering, ASME Trans., Volume 84, Series D, and No. 3 (1962):389-402.

[35] Schwa R. C. and Czyryc E. J. ,Effects of Notches and Saltwater Corrosion on the Flexural Fatigue Behavior of High-Strength Structural Alloys http://d.wanfangdata.com.cn/NSTLHY_NSTL_HY1287459.aspx

[36] Sasaki K., Isaacs H.S., Levy P.W., Transitions in electrochemical noise during pitting corrosion of aluminum in chloride environments, http://www.osti.gov/bridge/purl.cover.jsp?purl=/789436-zccqVv/native/

[37] McCafferty E.,Sequence of steps in the pitting of aluminum by chloride ions, Corrosion Science, Volume 45, Issue 7, (July 2003):1421-1438

[38] Rondelli G. and Vicentini B., Effect of copper on the localized corrosion resistance of Ni–Ti shape memory alloy, Biomaterials, Volume 23, Issue 3, (February 2002):639-644

[39] Ghidini T., Dalle Donne C., Fatigue life predictions using fracture mechanics methods, Engineering Fracture Mechanics 76 (2009):134–148

[40] Tang Yougen, Lu Lingbin, Roesky Herbert W., Wang Laiwe and Huang Baiyu, The effect of zinc on the aluminum anode of the aluminum–air battery, Journal of Power Sources Volume 138, Issues 1-2,(15 November 2004):313-318

[41] Governo A. T, Proença L., Parpot P., Lopes M. I. S. and Fonseca I. T. E., Electro-oxidation of D-xylose on platinum and gold electrodes in alkaline medium, Electrochimica Acta Volume 49, Issues 9-10, (15 April 2004):535-1545

[42] http://en.wikipedia.org/wiki/Cyclic_voltammetry

[43] Abdel -Gaber A.M., Abd-El-Nabey B.A., Sidahmed I.M, El-Zayady A.M.and. Saadaw M, Kinetics and thermodynamics of aluminum dissolution in 1.0 M sulphuric acid containing chloride ions, Materials Chemistry and Physics, Volume 98, Issues 2-3,(1 August 2006):291-297

[44] http://www.iom3.org/,Materials World, Vol. 12, No. 3, (March 2004):37-38, The Institute of Materials, Minerals and Mining.

[45] Broek David, Elementary Engineering Fracture Mechanics, 4th edition, Kluwer academic publisher.

[46] Jones Denny A., Principles and Prevention of corrosion, 2nd edition, Prentice-Hall.

[47] Mohanty J. R., PhD thesis, NIT Rourkela, India, (2006).

[48] Rokhlin S.I. , Kim J.Y, Nagy H., Zoofan B., Effect of pitting corrosion on fatigue crack initiation and fatigue life , Engineering Fracture Mechanics 62, (1999):425-444